



Department of Econometrics and Business Statistics

<http://monash.edu/business/ebs/research/publications>

Optimal forecast reconciliation with time series selection

Xiaoqian Wang, Rob J Hyndman, Shanika
L Wickramasuriya

October 2023

Working Paper no/yr



AACSB
ACCREDITED



Optimal forecast reconciliation with time series selection

Xiaoqian Wang

Monash University, VIC 3800, Australia

Email: xiaoqian.wang@monash.edu

Corresponding author

Rob J Hyndman

Monash University, VIC 3800, Australia

Email: rob.hyndman@monash.edu

Shanika L Wickramasuriya

Monash University, VIC 3145, Australia

Email: shanika.wickramasuriya@monash.edu

4 October 2023

Optimal forecast reconciliation with time series selection

Abstract

Forecast reconciliation ensures forecasts of time series in a hierarchy adhere to aggregation constraints, enabling aligned decision making. While forecast reconciliation can improve overall forecast accuracy in hierarchical structures, the most substantial improvements occur in series with initially poor base forecasts, and some series may still experience a deterioration in reconciled forecasts. In practice, some series in a hierarchy often have poor base forecasts due to inherent challenges that are hard to overcome. To address this, we propose two categories of forecast reconciliation methods that incorporate time series selection based on out-of-sample and in-sample information, respectively. Our methods keep “bad” base forecasts of some series unused in forming reconciled forecasts, preventing their negative influence on the reconciled forecasts. Additionally, this process adjusts the weights allocated to the remaining series when generating bottom-level reconciled forecasts. Moreover, our methods can reduce disparities arising from using different estimates of the base forecast error covariance matrix, thus alleviating the challenge of estimator selection. We evaluate the proposed methods through two simulation studies and two empirical applications using Australian domestic tourism data and labour force data, showing improved accuracy compared to alternative methods, particularly when addressing model misspecification.

Keywords: Hierarchical time series, Grouped time series, Linear forecast reconciliation, Optimization problem, Time series selection

1 Introduction

Hierarchical time series are characterized as a set of time series organized in a hierarchical aggregation structure, while grouped time series arise when attributes of interest are crossed rather than nested in the aggregation structure (Hyndman, Lee & Wang 2016). For example, consider the unemployment data, a crucial social and economic indicator, it is valuable to examine attributes such as labour market region and the length of time that unemployed people have been looking for work. Forecasts of time series in a given hierarchy should adhere to some

known aggregation constraints to maintain coherence, which is a crucial aspect for aligned decision making.

Earlier studies perform forecast reconciliation by focusing only on a single hierarchy level, subsequently aggregating or disaggregating their forecasts to produce coherent forecasts for other levels of the structure. These single-level methods typically fall into three categories, namely bottom-up (Dunn, Williams & Dechaine 1976), top-down (Gross & Sohl 1990), and middle-out (Athanasopoulos, Ahmed & Hyndman 2009). However, these methods only use information from a single level while overlooking valuable insights available at other levels and the intricate relationships in the structure. For in-depth insights into their properties, refer to a recent review by Athanasopoulos et al. (2023).

To overcome these limitations, Hyndman et al. (2011) introduced a reconciliation approach using a linear regression model based on forecasts from all series within a hierarchy, resulting in a generalized least squares (GLS) solution. This method initially generates independent base forecasts for all series in a hierarchical structure and subsequently adjusts these base forecasts to make them coherent. Following this, further research has led to the modifications of the least squares-based reconciliation method in various frameworks, including cross-sectional hierarchy (Hyndman, Lee & Wang 2016; Wickramasuriya, Athanasopoulos & Hyndman 2019; Panagiotelis et al. 2021), temporal hierarchy (Athanasopoulos et al. 2017; Nystrup et al. 2020), and cross-temporal hierarchy (Di Fonzo & Girolimetto 2023). In particular, assuming unbiased base forecasts and reconciled forecasts, Wickramasuriya, Athanasopoulos & Hyndman (2019) proposed the minimum trace (MinT) method, which formulates the reconciliation problem as minimizing the trace of the covariance matrix of reconciled forecast error. These approaches have been demonstrated to produce coherent and potentially more accurate forecasts compared to traditional single-level methods in various empirical applications (see, for example, Taieb, Taylor & Hyndman 2021; Panagiotelis et al. 2021; Wickramasuriya 2023). Furthermore, Erven & Cugliari (2015), Wickramasuriya, Athanasopoulos & Hyndman (2019), and Panagiotelis et al. (2021) provided theoretical insights into the performance of forecast reconciliation methods.

Although reconciliation is well acknowledged for its ability to improve overall forecast accuracy in hierarchical structures, it is important to acknowledge that reconciled forecasts for some series in the hierarchy may experience deterioration. As demonstrated by Athanasopoulos et al. (2017), most of the improvements attributed to reconciliation are observed in series with initially poor-performing base forecasts. Thus, they suggested that the ideal solution would be to combine the most accurate aspects of base forecasts from each level, aiming to avoid a myopic view from

a single level. In practice, it is not uncommon for some series in a hierarchy to exhibit poor performance in their base forecasts due to inherent challenges that are difficult to completely mitigate in real-world situations. These challenges may include model misspecification or low forecastability resulting from the absence of discernible patterns. In such cases, it becomes crucial to exclude “bad” base forecasts of some series in a hierarchy when performing reconciliation, thereby preventing their negative influence on the reconciled forecasts. This forms the primary objective of this paper.

This paper addresses a few gaps in the field of forecast reconciliation. First, we propose forecast reconciliation methods that incorporate time series selection based on out-of-sample information, assuming unbiased base forecasts. We formulate this as an optimization problem, using different penalty functions designed to control the number of nonzero column entries in the weighting matrix for linear forecast reconciliation. We theoretically show that the number of selected time series is at least equal to the number of series at the bottom level, and we can reconstruct the full hierarchical structure by aggregating/disaggregating the selected series. Second, we relax the unbiasedness assumption and introduce a reconciliation method with selection, utilizing in-sample observations and fitted values. This allows us to use the in-sample reconciliation performance for selection purposes. In this case, it may happen that less than the number of series at the bottom level are used for reconciliation. Third, we carry out simulation experiments and two empirical applications, showing that our proposed methods guaranteed coherent forecasts that outperformed or, at the very least, matched their respective benchmark methods. Finally, a remarkable feature of the proposed methods is their ability to reduce the disparities arising from using different estimates of the base forecast error covariance matrix, thereby mitigating the challenges associated with estimator selection, which is a prominent issue within the field of forecast reconciliation research.

The remainder of the paper is structured as follows. Section 2 presents the notations and a review of linear forecast reconciliation methods. Section 3 introduces our proposed methods to achieve time series selection in reconciliation, and provides some theoretical insights. Section 4 and Section 5 show the results from simulations and real-world datasets, respectively, followed by concluding remarks in Section 6. The R code for reproducing the results is available at [LINK](#).

2 Preliminaries

2.1 Notation

We denote the set $\{1, \dots, k\}$ by $[k]$ for any non-negative integer k . A *hierarchical time series* can be considered as an n -dimensional multivariate time series, $\{\mathbf{y}_t, t \in [T]\}$, that adheres to known linear constraints. Let $\mathbf{y}_t \in \mathbb{R}^n$ be a vector comprising observations of all time series in the hierarchy at time t , and $\mathbf{b}_t \in \mathbb{R}^{n_b}$ be a vector comprising observations of all bottom-level time series at time t . The full hierarchy at time t can be written as

$$\mathbf{y}_t = \mathbf{S}\mathbf{b}_t,$$

where \mathbf{S} is an $n \times n_b$ *summing matrix* that shows aggregation constraints present in the structure.

We can write the summing matrix as $\mathbf{S} = \begin{bmatrix} \mathbf{A} \\ \mathbf{I}_{n_b} \end{bmatrix}$, where \mathbf{A} is an $n_a \times n_b$ *aggregation matrix* with $n = n_a + n_b$, and \mathbf{I}_{n_b} is an n_b -dimensional identity matrix.

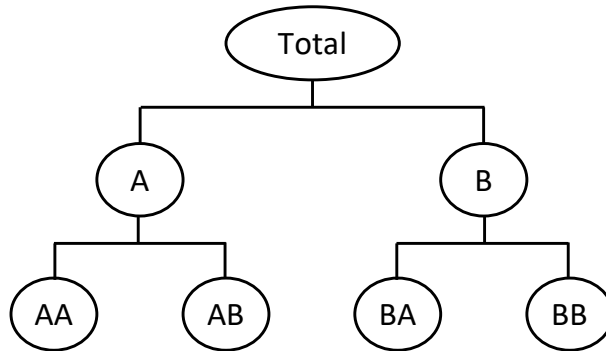


Figure 1: An example of a two-level hierarchical time series.

To clarify these notations, consider the example of the hierarchy in Figure 1. For this two-level hierarchy, $n = 7$, $n_b = 4$, $n_a = 3$, $\mathbf{y}_t = [y_{\text{Total},t}, y_{A,t}, y_{B,t}, y_{AA,t}, y_{AB,t}, y_{BA,t}, y_{BB,t}]'$, $\mathbf{b}_t = [y_{AA,t}, y_{AB,t}, y_{BA,t}, y_{BB,t}]'$, and

$$\mathbf{S} = \begin{bmatrix} 1 & 1 & 1 & 1 \\ 1 & 1 & 0 & 0 \\ 0 & 0 & 1 & 1 \\ & & & \mathbf{I}_4 \end{bmatrix}.$$

When data structure does not naturally disaggregate in a unique hierarchical manner, we can combine these hierarchical structures to form a *grouped time series*. Thus, grouped time series can

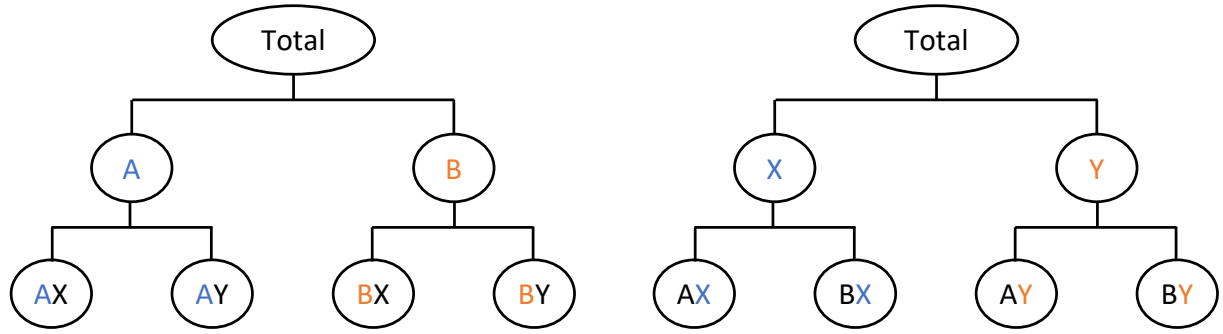


Figure 2: An example of a two level grouped time series.

also be considered as hierarchical time series with more than one grouping structure. Figure 2 shows an example of a two level grouped time series with two alternative aggregation structures. For this example, $n = 9$, $n_b = 4$, $n_a = 5$, $\mathbf{y}_t = [y_{\text{Total},t}, y_{A,t}, y_{B,t}, y_{X,t}, y_{Y,t}, y_{AX,t}, y_{AY,t}, y_{BX,t}, y_{BY,t}]'$, $\mathbf{b}_t = [y_{AX,t}, y_{AY,t}, y_{BX,t}, y_{BY,t}]'$, and

$$\mathbf{S} = \begin{bmatrix} 1 & 1 & 1 & 1 \\ 1 & 1 & 0 & 0 \\ 0 & 0 & 1 & 1 \\ 1 & 0 & 1 & 0 \\ 0 & 1 & 0 & 1 \\ & & \mathbf{I}_4 \end{bmatrix}.$$

2.2 Linear forecast reconciliation

Let $\hat{\mathbf{y}}_{T+h|T} \in \mathbb{R}^n$ be a vector of h -step-ahead *base forecasts* for all time series in the hierarchy, given observations up to time T , and stacked in the same order as \mathbf{y}_t . We can use any method to generate these forecasts, but In general they will not add up especially when we forecast each series independently.

When forecasting hierarchical time series, we expect the forecasts to be *coherent* (i.e., aggregation constraints are satisfied). Let $\tilde{\mathbf{y}}_{T+h|T} \in \mathbb{R}^n$ denote a vector of h -step-ahead *reconciled forecasts* which are coherent by construction, ψ a mapping that reconciles base forecasts, $\hat{\mathbf{y}}_{T+h|T}$. Then we have *forecast reconciliation* $\tilde{\mathbf{y}}_{T+h|T} = \psi(\hat{\mathbf{y}}_{T+h|T})$, which is essentially a post-processing method. In this paper, we focus on linear forecast reconciliation given by

$$\tilde{\mathbf{y}}_{T+h|T} = \mathbf{S}\mathbf{G}_h\hat{\mathbf{y}}_{T+h|T},$$

where

- G_h is an $n_b \times n$ weighting matrix that maps the base forecasts into the bottom level. In other words, it combines all base forecasts to form reconciled forecasts for bottom-level series.
- S is an $n \times n_b$ summing matrix that sums up bottom-level reconciled forecasts to produce coherent forecasts of all levels. It identifies the linear constraints involved in the hierarchy.

2.2.1 Minimum trace reconciliation

Let the h -step-ahead *base forecast errors* be defined as $\hat{e}_{T+h|T} = y_{T+h} - \hat{y}_{T+h|T}$, and the h -step-ahead *reconciled forecast errors* be defined as $\tilde{e}_{T+h|T} = y_{T+h} - \tilde{y}_{T+h|T}$. Wickramasuriya, Athanasopoulos & Hyndman (2019) formulated a linear reconciliation problem as minimizing the trace (MinT) of the h -step-ahead covariance matrix of the reconciled forecast errors, $\text{Var}(\tilde{e}_{T+h|T})$. Under the assumption of unbiasedness, the unique solution of the minimization problem is given by

$$G_h = \left(S' W_h^{-1} S \right)^{-1} S' W_h^{-1}, \quad (1)$$

where W_h is the positive definite covariance matrix of the h -step-ahead base forecast errors, $\text{Var}(\hat{e}_{T+h|T})$.

The trace minimization problem can be reformulated as a least squares problem with linear constraints given by

$$\begin{aligned} \min_{\tilde{y}_{T+h|T}} \quad & \frac{1}{2} (\hat{y}_{T+h|T} - \tilde{y}_{T+h|T})' W_h^{-1} (\hat{y}_{T+h|T} - \tilde{y}_{T+h|T}) \\ \text{s.t.} \quad & \tilde{y}_{T+h|T} = S \tilde{b}_{T+h|T}, \end{aligned} \quad (2)$$

where $\tilde{b}_{T+h|T} \in \mathbb{R}^{n_b}$ is the vector comprising h -step-ahead bottom-level reconciled forecasts, made at time T . Focusing on W_h , the intuitive behind the MinT reconciliation is that the larger the estimated variance of the base forecast errors, the larger the range of adjustments permitted for forecast reconciliation.

It's challenging to estimate W_h , especially for $h > 1$. Assuming that $W_h = k_h W_1, \forall h$, where $k_h > 0$, the MinT solution of G does not change with the forecast horizon, h . Hence, we will drop the subscript h for the ease of exposition. The most popularly used candidate estimators for W in the forecast reconciliation literature are listed as follows.

1. $\mathbf{W}_{OLS} = \mathbf{I}$ is the *OLS estimator* proposed by Hyndman et al. (2011), assuming that the base forecast errors are uncorrelated and equivariant. In what follows, we denote this as **OLS**.
2. $\mathbf{W}_{WLSs} = \text{diag}(\mathbf{S1})$ is the *WLS estimator applying structural scaling* proposed by Athanasopoulos et al. (2017). This estimator depends only on the aggregation structure of the hierarchy. It assumes that the variance of each bottom-level base forecast error is equivalent and uncorrelated between nodes. We denote this method as **WLSs**.
3. $\mathbf{W}_{WLSv} = \text{diag}(\hat{\mathbf{W}}_1)$ is the *WLS estimator applying variance scaling* proposed by Hyndman, Lee & Wang (2016), where $\hat{\mathbf{W}}_1$ denotes the unbiased covariance estimator based on the in-sample one-step-ahead base forecast errors (i.e., residuals). In the results that follow, we denote this as **WLSv**.
4. $\mathbf{W}_{MinT} = \hat{\mathbf{W}}_1$ is referred to as the *MinT estimator* based on the sample covariance matrix proposed by Wickramasuriya, Athanasopoulos & Hyndman (2019). We denote this method as **MinT** in the results that follow.
5. $\mathbf{W}_{MinTs} = \lambda \text{diag}(\hat{\mathbf{W}}_1) + (1 - \lambda)\hat{\mathbf{W}}_1$ is the *MinT shrinkage estimator* suggested by Wickramasuriya, Athanasopoulos & Hyndman (2019), in which off-diagonal elements of $\hat{\mathbf{W}}_1$ are shrunk toward zero. We refer to this method as **MinTs**.

It's hard to say which estimator for \mathbf{W} works better. Pritularga, Svetunkov & Kourentzes (2021) demonstrated that the performance of forecast reconciliation is affected by two sources of uncertainties, i.e., the base forecast uncertainty and the reconciliation weight uncertainty. Recall that the uncertainty in the MinT solution in Equation 1 is introduced by the uncertainty in the reconciliation weighting matrix as the summing matrix is fixed for a certain hierarchy. This indicates that OLS and WLSs estimators for \mathbf{W} may lead to less volatile reconciliation performance compared to WLSv, MinT, and MinTs estimators. Panagiotelis et al. (2021) provided a geometric intuition for reconciliation and showed that, when considering the Euclidean distance loss function, OLS reconciliation yields results that are at least as favorable as the base forecasts, whereas MinT reconciliation performs poorly relative to the base forecasts. However, when considering the mean squared reconciled forecast error, Wickramasuriya (2021) indicated that MinT reconciliation is better than OLS reconciliation. Therefore, which estimator for \mathbf{W} to use hinges on the specific hierarchical time series of interest, the targeted level or series, and the selected loss function.

2.2.2 Relaxation of the unbiasedness assumptions

Both Hyndman et al. (2011) and Wickramasuriya, Athanasopoulos & Hyndman (2019) impose two unbiasedness conditions, i.e., the base forecasts and the reconciled forecasts are unbiased.

Ben Taieb & Koo (2019) proposed a reconciliation method relaxing the assumption of unbiasedness. Specifically, by expanding the training window forward by one observation until $T - h$, they formulated the reconciliation problem as a regularized empirical risk minimization (RERM) problem given by

$$\min_{\mathbf{G}_h} \frac{1}{(T - T_1 - h + 1)n} \|\mathbf{Y}_h^* - \hat{\mathbf{Y}}_h^* \mathbf{G}_h' \mathbf{S}'\|_F^2 + \lambda \|\text{vec}(\mathbf{G}_h)\|_1,$$

where T_1 denotes the minimum number of observations used for model training, $\|\cdot\|_F$ is the Frobenius norm, $\mathbf{Y}_h^* = [\mathbf{y}_{T_1+h}, \dots, \mathbf{y}_T]' \in \mathbb{R}^{(T-T_1-h+1) \times n}$, $\hat{\mathbf{Y}}_h^* = [\hat{\mathbf{y}}_{T_1+h|T_1}, \dots, \hat{\mathbf{y}}_{T|T-h}]' \in \mathbb{R}^{(T-T_1-h+1) \times n}$, and $\lambda \geq 0$ is a regularization parameter.

When $\lambda = 0$, the problem reduces to an empirical risk minimization (ERM) problem without regularization. Assuming that the series in the hierarchy are jointly weakly stationary and $\hat{\mathbf{Y}}_h^{*'} \hat{\mathbf{Y}}_h^*$ is invertible, it has a closed-form solution given by

$$\hat{\mathbf{G}}_h = \mathbf{B}_h^{*'} \hat{\mathbf{Y}}_h^* (\hat{\mathbf{Y}}_h^{*'} \hat{\mathbf{Y}}_h^*)^{-1},$$

where $\mathbf{B}_h^* = [\mathbf{b}_{T_1+h}, \dots, \mathbf{b}_T]' \in \mathbb{R}^{(T-T_1-h+1) \times n}$. If $\hat{\mathbf{Y}}_h^{*'} \hat{\mathbf{Y}}_h^*$ is not invertible, they suggested using a generalized inverse.

When $\lambda > 0$, imposing such a L_1 penalty on \mathbf{G}_h will introduce sparsity and reduce estimation variance, albeit at the cost of introducing some bias. In addition, they also proposed another strategy that penalizes the matrix \mathbf{G}_h towards the solution obtained by bottom-up method, i.e., $\mathbf{G}_{\text{BU}} = [\mathbf{0}_{n_b \times n_a} \mid \mathbf{I}_{n_b}]$.

Following the work, Wickramasuriya (2021) proposed an empirical MinT (**EMinT**) without the unbiasedness constraint by minimizing the trace of the covariance matrix of the reconciled forecast errors, $\text{Var}(\tilde{\mathbf{e}}_{T+h|T})$. Assuming that the series are jointly weakly stationary, she derived the solution given by

$$\hat{\mathbf{G}}_h = \mathbf{B}_h' \hat{\mathbf{Y}}_h (\hat{\mathbf{Y}}_h' \hat{\mathbf{Y}}_h)^{-1},$$

where $\mathbf{B}_h = [\mathbf{b}_h, \dots, \mathbf{b}_T]' \in \mathbb{R}^{(T-h+1) \times n}$, and $\hat{\mathbf{Y}}_h = [\hat{\mathbf{y}}_{h|0}, \dots, \hat{\mathbf{y}}_{T|T-h}]' \in \mathbb{R}^{(T-h+1) \times n}$. The difference between EMinT and ERM lies in the data sources used, as EMinT uses in-sample observations and base forecasts, while ERM relies on observations and base forecasts from

a holdout validation set. We note that both ERM and EMinT consider an estimate of G that changes over the forecast horizon, which is why we keep the subscript h here.

In practice, a prevalent challenge in forecast reconciliation arises when the base forecasts of some time series within the hierarchical structure may perform poorly, especially for large hierarchies. This can be attributed to either the inherent complexity of forecasting these series or potential model misspecification. In such cases, the effectiveness of forecast reconciliation may diminish, as the role of the weighting matrix G is to assimilate *all* base forecasts and map them into bottom-level disaggregated forecasts which are subsequently summed by S . While the RERM method proposed by Ben Taieb & Koo (2019) introduces sparsity by shrinking some elements of G towards zero, it remains incapable of mitigating the adverse impact of underperforming base forecasts on the quality of the reconciled forecasts. Moreover, the method is time-consuming because it uses expanding windows to recursively generate out-of-sample base forecasts, which are then used in the minimization problem.

We therefore propose two branches of innovative methods, constrained (out-of-sample-based) and unconstrained (in-sample-based) reconciliation with selection. These methods aim to identify and address the negative effect of some base forecasts of poor performance in a hierarchy on the overall performance of the reconciled forecasts. Additionally, through the incorporation of regularization in our objective function, our method has the potential to enhance reconciliation outcomes produced by using a “bad” choice of W , thus reducing the risk of choosing estimator of W . Moreover, our method generalizes to grouped hierarchies.

3 Forecast reconciliation with time series selection

In this section, we introduce our methods for keeping forecasts of an automatically selected set of series, identified as harmful to reconciliation, unused in forming reconciled forecasts, i.e., forecast reconciliation with series selection. Section 3.1 introduces constrained reconciliation methods with selection that formulate the problem based on out-of-sample base forecasts, while Section 3.2 presents an unconstrained reconciliation method with selection that formulates the problem based on in-sample observations and base forecasts.

3.1 Series selection with unbiasedness constraint

As S is fixed and $\hat{y}_{T+h|T}$ is given, the estimation of G carries the linear reconciliation performance, as shown in Equation 1. (Subscript h is dropped as we assume W and G do not change over

the forecast horizon.) A natural way to keep forecasts of some series unused in reconciliation is through controlling the number of nonzero column entries in G . This leads to a generalization of the MinT optimization problem by applying an additional penalty to the objective function. More precisely, we consider the optimization problem given by

$$\begin{aligned} \min_{\mathbf{G}} \quad & \frac{1}{2} (\hat{\mathbf{y}}_{T+h|T} - \mathbf{S}\mathbf{G}\hat{\mathbf{y}}_{T+h|T})' \mathbf{W}^{-1} (\hat{\mathbf{y}}_{T+h|T} - \mathbf{S}\mathbf{G}\hat{\mathbf{y}}_{T+h|T}) + \lambda \mathbf{g}(\mathbf{G}) \\ \text{s.t.} \quad & \mathbf{G}\mathbf{S} = \mathbf{I}, \end{aligned} \quad (3)$$

where $\mathbf{g}(\cdot)$ is defined as an exterior penalty function designed to penalize the columns of \mathbf{G} towards zero, with λ is the corresponding penalty coefficient. Thus, this can be considered as a grouped variable selection problem, with each group corresponding to a column of \mathbf{G} . The constraint, $\mathbf{G}\mathbf{S} = \mathbf{I}$, reflects the assumption that base forecasts and reconciled forecasts are unbiased. When $\lambda = 0, \forall h$, the problem reduces to the MinT optimization problem in Equation 2 with a closed-form solution given by Equation 1.

Proposition 1. *Under the assumption of unbiasedness, the count of nonzero column entries of \mathbf{G} (i.e., the number of time series selected for reconciliation), derived through solving Equation 3, is at least equal to the number of time series at the bottom level. In addition, we can restore the full hierarchical structure by aggregating/disaggregating the selected time series.*

Proof. According to the unbiasedness constraint $\mathbf{G}\mathbf{S} = \mathbf{I}$, we have

$$\min (\text{rank}(\mathbf{G}), \text{rank}(\mathbf{S})) \geq \text{rank}(\mathbf{I}_{n_b}) = n_b,$$

which indicates that the count of nonzero column entries of \mathbf{G} is at least equal to n_b .

Let $\mathbf{X}_{\mathbf{S}} \in \mathbb{R}^{r \times |\mathbf{S}|}$ denote the submatrix of the $r \times c$ matrix \mathbf{X} with column indices forming a set \mathbf{S} (and when $\mathbf{S} = \{j\}$, we simply use $\mathbf{X}_{\cdot j}$). Here, $|\mathbf{S}|$ denotes the size of the set \mathbf{S} . Similarly, let $\mathbf{X}_{\mathbf{S}} \in \mathbb{R}^{|\mathbf{S}| \times c}$ denote the submatrix of \mathbf{X} whose rows are indexed by a set \mathbf{S} (and when $\mathbf{S} = \{i\}$, we simply use \mathbf{X}_i). Assuming that the set \mathbf{S} consists of the indices of nonzero columns in the solution of Equation 3, the following equations hold:

$$\begin{aligned} \mathbf{G}\mathbf{S} &= \mathbf{G}_{\cdot \mathbf{S}}\mathbf{S}_{\mathbf{S}} \text{ and} \\ \min (\text{rank}(\mathbf{G}_{\cdot \mathbf{S}}), \text{rank}(\mathbf{S}_{\mathbf{S}})) &\geq \text{rank}(\mathbf{I}_{n_b}) = n_b. \end{aligned}$$

Additionally, we have $\text{rank}(\mathbf{S}_{\mathbf{S}}) \leq n_b$ as \mathbf{S} has n_b columns. Therefore, we can conclude that $\text{rank}(\mathbf{S}_{\mathbf{S}}) = n_b$, which implies that the hierarchical structure can be fully restored by aggregating/disaggregating the selected time series, $(\mathbf{y}_t)_{\mathbf{S}}$.

For example, consider the simple hierarchy shown in Figure 1, it is not possible for our constrained reconciliation methods with selection to simultaneously zero out columns of \mathbf{G} associated with series AA and AB. However, it is possible to zero out columns related to series AA and BA simultaneously.

Proposition 2. *The optimization problem in Equation 3 can be reformulated as a least squares problem with regularization and linear equality constraint as follows:*

$$\begin{aligned} \min_{\text{vec}(\mathbf{G})} \quad & \frac{1}{2} \left(\hat{\mathbf{y}}_{T+h|T} - \left(\hat{\mathbf{y}}'_{T+h|T} \otimes \mathbf{S} \right) \text{vec}(\mathbf{G}) \right)' \mathbf{W}^{-1} \left(\hat{\mathbf{y}}_{T+h|T} - \left(\hat{\mathbf{y}}'_{T+h|T} \otimes \mathbf{S} \right) \text{vec}(\mathbf{G}) \right) + \lambda \mathbf{g}(\text{vec}(\mathbf{G})) \\ \text{s.t.} \quad & (\mathbf{S}' \otimes \mathbf{I}_{n_b}) \text{vec}(\mathbf{G}) = \text{vec}(\mathbf{I}_{nb}), \end{aligned} \quad (4)$$

which is characterized as a high-dimensional problem in which the number of features, denoted as $p = n_b \times n$, is much larger than the number of observations, n .

Proof. Let $\text{vec}(\mathbf{A})$ denote the vectorization of a matrix \mathbf{A} , which stacks the columns of \mathbf{A} on top of one another. We have

$$\begin{aligned} \text{vec}(\hat{\mathbf{y}}_{T+h|T}) &= \hat{\mathbf{y}}_{T+h|T}, \\ \text{vec}(\mathbf{S}\mathbf{G}\hat{\mathbf{y}}_{T+h|T}) &= \left(\hat{\mathbf{y}}'_{T+h|T} \otimes \mathbf{S} \right) \text{vec}(\mathbf{G}), \\ \text{vec}(\mathbf{G}\mathbf{S}) &= \text{vec}(\mathbf{I}_{nb}\mathbf{G}\mathbf{S}) = (\mathbf{S}' \otimes \mathbf{I}_{n_b}) \text{vec}(\mathbf{G}). \end{aligned}$$

Substituting the terms in Equation 3 with these expressions, the previous problem now takes the form of a regression problem with an additional regularization term and an equality constraint on the coefficients, as shown in Equation 4.

Moving forward, we present three classes of regularizations we use to establish forecast reconciliation with series selection, resulting in the consideration of three optimization problems: (i) group best-subset selection with ridge regularization, (ii) intuitive method with L_0 regularization, and (iii) group lasso method.

3.1.1 Group best-subset selection with ridge regularization

In high-dimensional regime with $p \gg n$, a common desiderata is to assume that the true regression coefficient (i.e., $\text{vec}(\mathbf{G})$ in our problem) is sparse. We propose to apply a combination of L_0 and L_2 regularization as the exterior penalty function to control the nonzero column entries in \mathbf{G} :

$$\begin{aligned} \min_{\text{vec}(\mathbf{G})} \quad & \frac{1}{2} \left(\hat{\mathbf{y}}_{T+h|T} - \left(\hat{\mathbf{y}}'_{T+h|T} \otimes \mathbf{S} \right) \text{vec}(\mathbf{G}) \right)' \mathbf{W}^{-1} \left(\hat{\mathbf{y}}_{T+h|T} - \left(\hat{\mathbf{y}}'_{T+h|T} \otimes \mathbf{S} \right) \text{vec}(\mathbf{G}) \right) \\ & + \lambda_0 \sum_{j=1}^n \mathbf{1}(\mathbf{G}_{\cdot j} \neq \mathbf{0}) + \lambda_2 \|\text{vec}(\mathbf{G})\|_2^2 \\ \text{s.t.} \quad & (\mathbf{S}' \otimes \mathbf{I}_{n_b}) \text{vec}(\mathbf{G}) = \text{vec}(\mathbf{I}_{nb}), \end{aligned} \quad (5)$$

where $\mathbf{1}(\cdot)$ is the indicator function, $\lambda_0 \geq 0$ controls the number of nonzero columns of \mathbf{G} selected, and $\lambda_2 \geq 0$ controls the strength of the ridge regularization. In a hierarchical time series context, the parameter of interest in Equation 5, $\text{vec}(\mathbf{G})$, has an inherent non-overlapping group structure, wherein each group corresponds to a single column of \mathbf{G} , each with a size of n_b . Therefore, we refer to this reconciliation method as *group best-subset selection with ridge regularization*. In the results that follow, we label the method differently based on various estimators for \mathbf{W} , referring to them as **OLS-subset**, **WLSs-subset**, **WLSv-subset**, **MinT-subset**, and **MinTs-subset**, respectively.

The inclusion of the ridge term in Equation 5 is motivated by earlier work on best-subset selection (e.g., Hazimeh & Mazumder 2020; Mazumder, Radchenko & Dedieu 2022), which suggests that additional ridge regularization can mitigate the poor predictive performance of best-subset selection method in the low signal-to-noise ratio (SNR) regimes.

We present a Big-M based mixed integer programming (MIP) formulation for problem in Equation 5 given by

$$\begin{aligned}
 & \min_{\text{vec}(\mathbf{G}), \mathbf{z}, \check{\mathbf{e}}, \mathbf{g}^+} \frac{1}{2} \check{\mathbf{e}}' \mathbf{W}^{-1} \check{\mathbf{e}} + \lambda_0 \sum_{j=1}^n z_j + \lambda_2 \mathbf{g}^{+'} \mathbf{g}^+ \\
 & \text{s.t.} \quad (\mathbf{S}' \otimes \mathbf{I}_{n_b}) \text{vec}(\mathbf{G}) = \text{vec}(\mathbf{I}_{n_b}) \\
 & \quad \hat{\mathbf{y}}_{T+h|T} - (\hat{\mathbf{y}}'_{T+h|T} \otimes \mathbf{S}) \text{vec}(\mathbf{G}) = \check{\mathbf{e}} \\
 & \quad \sum_{i=1}^{n_b} g_{i+(j-1)n_b}^+ \leq \mathcal{M} z_j, \quad j \in [n] \\
 & \quad \mathbf{g}^+ \geq \text{vec}(\mathbf{G}) \\
 & \quad \mathbf{g}^+ \geq -\text{vec}(\mathbf{G}) \\
 & \quad z_j \in \{0, 1\}, \quad j \in [n],
 \end{aligned} \tag{6}$$

where \mathcal{M} is a Big-M parameter (a-priori specified) that is sufficiently large such that some optimal solution, say \mathbf{g}^{+*} , to Equation 6 satisfies $\max_{j \in [n]} \sum_{i=1}^{n_b} g_{i+(j-1)n_b}^+ \leq \mathcal{M}$, the binary variable z_j controls whether all the regression coefficients, $\text{vec}(\mathbf{G})$, in group j are zero or not, i.e., $z_j = 0$ implies that $\mathbf{G}_{\cdot j} = \mathbf{0}$, and $z_j = 1$ implies that $\sum_{i=1}^{n_b} g_{i+(j-1)n_b}^+ \leq \mathcal{M}$. Such Big-M formulations are commonly used in MIP problems to model relations between discrete and continuous variables, and have been recently explored in regression with L_0 regularization, see Bertsimas, King & Mazumder (2016) for more discussion. The problem is a mixed integer quadratic program (MIQP) that can be solved using commercial MIP solvers, e.g., Gurobi and CPLEX.

Parameter tuning. $\lambda_0 \geq 0$ and $\lambda_2 \geq 0$ are tuning parameters. To avoid computationally-expensive cross-validation, we tune the parameters to minimize the sum of squared reconciled forecast errors on the truncated training set, comprising only the h observations closest to the forecast origin. Let $\lambda_0^1 = \frac{1}{2} (\hat{\mathbf{y}}_{T+h|T} - \hat{\mathbf{y}}_{T+h|T}^{\text{bench}})' \mathbf{W}^{-1} (\hat{\mathbf{y}}_{T+h|T} - \hat{\mathbf{y}}_{T+h|T}^{\text{bench}})$ that captures the scale of first term in the objective, where $\hat{\mathbf{y}}_{T+h|T}^{\text{bench}}$ is a vector of reconciled forecasts obtained using Equation 1 with same estimator of \mathbf{W} , and define $\lambda_0^k = 0.0001 \lambda_0^1$. For the parameter λ_0 , we consider a grid of $k + 1$ values, $\{\lambda_0^1, \dots, \lambda_0^k, 0\}$, where $\lambda_0^j = \lambda_0^1 (\lambda_0^k / \lambda_0^1)^{(j-1)/(k-1)}$ for $j \in [k]$. So $\lambda_0^1, \dots, \lambda_0^k$ is a sequence decreasing on the log scale. We use a grid of six values for the parameter λ_2 , $\{0, 10^{-2}, 10^{-1}, 10^0, 10^1, 10^2\}$. Therefore, we tune over a two-dimensional grid of $(k + 1) \times 6$ values to find the optimal combination of λ_0 and λ_2 .

Computation details. The MIQP problem in Equation 6 is NP-Hard and computationally intensive. Bertsimas, King & Mazumder (2016) showed that commercial MIP solvers are capable of tackling problem instances for p up to a thousand. To address larger instances, there has been impressive work on developing MIP-based approaches for solving L_0 -regularized regression

problem, e.g., Bertsimas, King & Mazumder (2016), Hazimeh & Mazumder (2020), and Hazimeh, Mazumder & Saab (2022). However, it is challenging to extend their approaches to accommodate additional constraints within the optimization problem. Despite the potential sluggishness of handling large instances with commercial MIP solvers, in our experiments, we use Gurobi to solve our problem in Equation 6 by configuring parameters such as $\text{MIPGap} = 0.001$ and $\text{TimeLimit} = 600$ seconds for cases with $p > 1000$. This enables us to terminate the solver before reaching the global optimum and return a suboptimal solution instead. This strategy is motivated by our need to consider numerous parameter candidates, and the final solution will be validated against the training set, which helps prevent the utilization of a very poor estimate of G .

3.1.2 Intuitive method with L_0 regularization

Instead of estimating the entire matrix G in Section 3.1.1, we leverage the MinT solution in Equation 1 to streamline the optimization problem under consideration. Specifically, we define $\bar{S} = AS$, where $A = \text{diag}(z)$ is an $n \times n$ diagonal matrix, and z is an n -dimensional vector with elements either equal to 0 or 1. Taking the MinT solution in Equation 1, we have $\bar{G} = (S'A'W^{-1}AS)^{-1}S'A'W^{-1}$. Given fixed S and estimation of W , \bar{G} is entirely determined by A . By this way, when the j th diagonal element of A equals zero, the j th column of \bar{G} becomes entirely composed of zeros. Therefore, the optimization problem can be reduced to an integer quadratic programming (IQP) problem in which all of the variables are restricted to be integers:

$$\begin{aligned} \min_A \quad & \frac{1}{2} (\hat{y}_{T+h|T} - S\bar{G}\hat{y}_{T+h|T})' W^{-1} (\hat{y}_{T+h|T} - S\bar{G}\hat{y}_{T+h|T}) + \lambda_0 \sum_{j=1}^n A_{jj} \\ \text{s.t.} \quad & \bar{G} = (S'A'W^{-1}AS)^{-1}S'A'W^{-1} \\ & \bar{G}S = I, \end{aligned}$$

where $\lambda_0 \geq 0$ controls the number of nonzero diagonal elements in A , consequently affecting the number of nonzero columns (i.e., selected time series) in G . We refer to this reconciliation method as *intuitive method with L_0 regularization*. In the results that follow, we label the method differently based on various estimators for W , referring to them as **OLS-intuitive**, **WLSs-intuitive**, **WLSv-intuitive**, **MinT-intuitive**, and **MinTs-intuitive**, respectively.

We should note that implementing grouped variable selection with this optimization problem can be challenging because it imposes restrictions on the parameter of interest (\bar{G}) to ensure it

adheres rigorously to the analytical solution of MinT while making the selection. Therefore, the resulting solution may not have zero columns.

To ensure the invertibility of $S'A'W^{-1}AS$ and make the problem compatible with Gurobi, we reformulate the problem as

$$\begin{aligned}
 \min_{A, \bar{G}, C, \check{e}, z} \quad & \frac{1}{2} \check{e}' W^{-1} \check{e} + \lambda_0 \sum_{j=1}^n z_j \\
 \text{s.t.} \quad & \bar{G}S = I \\
 & \hat{y}_{T+h|T} - (\hat{y}'_{T+h|T} \otimes S) \text{vec}(\bar{G}) = \check{e} \\
 & \bar{G}AS = I \\
 & \bar{G} = CS'A'W^{-1} \\
 & z_j \in \{0, 1\}, \quad j \in [n].
 \end{aligned} \tag{7}$$

Parameter tuning. Similarly to the setup in Section 3.1.1, we select the tuning parameter, λ_0 , by minimizing the sum of squared reconciled forecast errors on a truncated training set, comprising only the h observations occurred prior to the forecast origin. Let $\lambda_0^1 = \frac{1}{2} (\hat{y}_{T+h|T} - \hat{y}_{T+h|T}^{\text{bench}})' W^{-1} (\hat{y}_{T+h|T} - \hat{y}_{T+h|T}^{\text{bench}})$, and $\lambda_0^k = 0.0001\lambda_0^1$, the collection of candidate values for λ_0 we consider is $\{\lambda_0^1, \dots, \lambda_0^k, 0\}$, where $\lambda_0^j = \lambda_0^1 (\lambda_0^k / \lambda_0^1)^{(j-1)/(k-1)}$ for $j \in [k]$.

Computation details. Following a setup akin to that in Section 3.1.1, we employ Gurobi to solve Equation 7 by configuring parameters such as MIPGap = 0.001 and TimeLimit = 600 seconds for problems with $p > 1000$.

3.1.3 Group lasso method

Lasso is another popular method for selection and estimation of parameters in the context of linear regression. Yuan & Lin (2006) introduced the group lasso method that can be used when there is a grouped structure among the variables. Here, we consider a *group lasso problem under the unbiasedness assumption* given by

$$\begin{aligned}
 \min_G \quad & \frac{1}{2} \left(\hat{y}_{T+h|T} - (\hat{y}'_{T+h|T} \otimes S) \text{vec}(G) \right)' W^{-1} \left(\hat{y}_{T+h|T} - (\hat{y}'_{T+h|T} \otimes S) \text{vec}(G) \right) \\
 & + \lambda \sum_{j=1}^n w_j \|G_{\cdot j}\|_2 \\
 \text{s.t.} \quad & (S' \otimes I_{n_b}) \text{vec}(G) = \text{vec}(I_{n_b}),
 \end{aligned} \tag{8}$$

where $\lambda \geq 0$ is a tuning parameter, $w_j \neq 0$ is the penalty weight assigned in G_j to make model more flexible, and the second term in the objective is the penalty function that is intermediate between the L_1 -penalty that is used in the lasso and the L_2 -penalty that is used in ridge regression. In the results that follow, we label the method differently based on various estimators for W , referring to them as **OLS-lasso**, **WLSs-lasso**, **WLSv-lasso**, **MinT-lasso**, and **MinTs-lasso**, respectively.

Next, we present the second order cone programming (SOCP) formulation for the group lasso based estimators given by

$$\begin{aligned}
 \min_{\text{vec}(G), \check{e}, g^+} \quad & \frac{1}{2} \check{e}' W_h^{-1} \check{e} + \lambda \sum_{j=1}^n w_j c_j \\
 \text{s.t.} \quad & (S' \otimes I_{n_b}) \text{vec}(G) = \text{vec}(I_{n_b}) \\
 & \hat{y}_{T+h|T} - (\hat{y}'_{T+h|T} \otimes S) \text{vec}(G) = \check{e} \\
 & c_j = \sqrt{\sum_{i=1}^{n_b} g_{i+(j-1)n_b}^2}, \quad j \in [n].
 \end{aligned} \tag{9}$$

Equation 9 includes additional auxiliary variables $c_j \in \mathbb{R}_{\geq 0}$, $j \in [n]$, and second order cone constraints, $c_j = \sqrt{\sum_{i=1}^{n_b} g_{i+(j-1)n_b}^2}$ for $j \in [n]$.

Compared to the previous two methods we proposed, the group lasso method is computationally friendlier. Nonetheless, Hazimeh, Mazumder & Radchenko (2023) demonstrated, both empirically and theoretically, that group L_0 -regularized method exhibits advantages over its group lasso counterpart across a range of regimes. Group lasso can either be highly dense or possess non-zero coefficients that are overly shrunk. This issue becomes more pronounced when the groups are correlated with each other as group lasso tends to retain all correlated groups instead of seeking a more concise model.

Penalty weights and parameter tuning. In the context of group lasso, the default choice for the penalty weight, w_j , is $\sqrt{p_j}$, where p_j is the size of each group (in our case, $p_j = n_b$). In our experiment, we allocate different penalty weights to each group by considering $w_j = 1 / \left\| G_j^{\text{bench}} \right\|_2$, which allows us to account for variations in scale across different levels in the hierarchy.

We compute the group lasso over $k + 1$ values of the tuning parameter λ , and select the tuning parameter by optimizing the sum of squared reconciled forecast errors on a truncated training set, consisting only of h observations occurred prior to the forecast origin. The collection of candidate values for λ under consideration is $\{\lambda^1, \dots, \lambda^k, 0\}$,

where $\lambda^1 = \max_{j=1,\dots,n} \left\| - \left(\left(\hat{\mathbf{y}}'_{T+h|T} \otimes \mathbf{S} \right)_{\cdot j^*} \right)' \mathbf{W}^{-1} \hat{\mathbf{y}}_{T+h|T} \right\|_2 / w_j$, $\lambda^k = 0.0001 \lambda^1$, and $\lambda^j = \lambda^1 (\lambda^k / \lambda^1)^{(j-1)/(k-1)}$ for $j \in [k]$.

Proposition 3. *Ignoring the unbiasedness constraint, we define λ^1 as the smallest λ value such that all predictors in the group lasso problem have zero coefficients. Then we have*

$$\lambda^1 = \max_{j=1,\dots,n} \left\| - \left(\left(\hat{\mathbf{y}}'_{T+h|T} \otimes \mathbf{S} \right)_{\cdot j^*} \right)' \mathbf{W}^{-1} \hat{\mathbf{y}}_{T+h|T} \right\|_2 / w_j,$$

where j^* denotes the column index of $\hat{\mathbf{y}}'_{T+h|T} \otimes \mathbf{S}$ that corresponds to the j th column of \mathbf{G} .

Proof. Denote $\boldsymbol{\beta} = \text{vec}(\mathbf{G})$, and the first term in the objective of Equation 8 as $L(\boldsymbol{\beta} \mid \mathbf{D})$, where \mathbf{D} is the working data $\{\hat{\mathbf{y}}_{T+h|T}, \hat{\mathbf{y}}'_{T+h|T} \otimes \mathbf{S}\}$. Ignoring the unbiasedness constraint, we define λ^1 as the smallest λ value such that all predictors in the group lasso problem have zero coefficients, i.e., the solution at λ^1 is $\hat{\boldsymbol{\beta}}^1 = \mathbf{0}$. (Note that there is no intercept in our problem.) Under the Karush-Kuhn-Tucker conditions, we have

$$\begin{aligned} \lambda^1 &= \max_{j=1,\dots,n} \left\| \left[\nabla L(\hat{\boldsymbol{\beta}}^1 \mid \mathbf{D}) \right]^{(j)} \right\|_2 / w_j \\ &= \max_{j=1,\dots,n} \left\| - \left(\left(\hat{\mathbf{y}}'_{T+h|T} \otimes \mathbf{S} \right)_{\cdot j^*} \right)' \mathbf{W}^{-1} \hat{\mathbf{y}}_{T+h|T} \right\|_2 / w_j. \end{aligned}$$

Computation details. Due to the incorporation of the unbiasedness constraint, we can not directly use some open-source packages designed for group lasso. Consequently, we employ Gurobi to solve the SOCP problem in Equation 9, configuring it by setting OptimalityTol = 0.0001.

3.2 Series selection method without unbiasedness constraint

In this section, we relax the unbiasedness constraint, $\mathbf{GS} = \mathbf{I}$, and introduce a reconciliation method with selection that relies on in-sample observations and fitted values. Let $\mathbf{Y} \in \mathbb{R}^{T \times n}$ denote a matrix comprising observations from all time series on the training set in the structure, and $\hat{\mathbf{Y}} \in \mathbb{R}^{T \times n}$ denote a matrix of in-sample one-step-ahead forecasts (i.e., fitted values) for all time series, where T is the length of the training set. The proposed *empirical group lasso* method considers the optimization problem given by

$$\min_{\mathbf{G}} \quad \frac{1}{2T} \|\mathbf{Y} - \hat{\mathbf{Y}} \mathbf{G}' \mathbf{S}'\|_F^2 + \lambda \sum_{j=1}^n w_j \|\mathbf{G}_{\cdot j}\|_2,$$

where $\|\cdot\|_F$ is the Frobenius norm, and $\lambda \geq 0$ is a tuning parameter, $w_j \neq 0$ is the penalty weight assigned in G_j to make a more flexible model. Following the work by Ben Taieb & Koo (2019), using the fact that $\|X\|_F^2 = \|\text{vec}(X)\|_2^2$ and the useful formulation that $\text{vec}(ABC) = (C' \otimes A) \text{vec}(B)$, we rewrite the problem as

$$\min_{\text{vec}(G)} \frac{1}{2N} \|\text{vec}(Y) - (S \otimes \hat{Y}) \text{vec}(G')\|_2^2 + \lambda \sum_{j=1}^n w_j \|G_j\|_2,$$

which becomes a standard group lasso problem, with $\text{vec}(Y)$ serving as the dependent variable and $S \otimes \hat{Y}$ as the covariate matrix. We denote this as **Elasso** in the results that follow.

Upon relaxing the unbiasedness constraint, the number of non-zero column entries in the solution for G may be less than the number of time series at the bottom level. This differs from the series selection methods with an unbiasedness constraint that we introduced in Section 3.1. In an extreme scenario, the solution may take the form of a top-down $G_{TD} = [p \mid O_{n_b \times (n-1)}]$, where only the column corresponding to the top level (most aggregated level) retains non-zero values, and $p = (p_1, p_2, \dots, p_{n_b})$ is a proportionality vector obtained based on in-sample reconciled forecast errors such that $\sum_{i=1}^{n_b} p_i = 1$.

We also explored the empirical version of group best-subset selection with ridge regularization and intuitive method with L_0 regularization in which we do not impose the unbiasedness constraint. It is worth mentioning that Hazimeh, Mazumder & Radchenko (2023) presented a new algorithmic framework for formulating the group L_0 problem with ridge regularization and provided the **L0Group** Python package¹ for implementation. However, our experiments showed that this algorithm can not terminate within five hours for typical instances with $p \sim 10^4$. Therefore, in this paper, we only present the empirical group lasso method for series selection without unbiasedness constraint.

Penalty weights and parameter tuning. Similarly to the setup in Section 3.1.3, we assign different penalty weights to each group by setting $w_j = 1 / \|G_j^{\text{OLS}}\|_2$, where G^{OLS} is the solution obtained by the OLS estimator of W . We select the tuning parameter, λ , by minimizing the sum of squared reconciled forecast errors on a truncated training set, comprising only the h observations closest to the forecast origin. Specifically, we form the set of candidate values for λ as $\{\lambda^1, \dots, \lambda^k, 0\}$, where $\lambda^1 = \max_{j=1, \dots, n} \left\| -\frac{1}{N} \left((S \otimes \hat{Y})_{j*} \right)' \text{vec}(Y) \right\|_2 / w_j$, $\lambda^k = 0.0001\lambda^1$, and $\lambda^j = \lambda^1 (\lambda^k / \lambda^1)^{(j-1)/(k-1)}$ for $j \in [k]$. Following the same derivation as in the proof of

¹The L0Group Python package is available on github at <https://github.com/hazimehh/L0Group>.

Proposition 3, λ^1 is the smallest λ value such that all predictors in the empirical group lasso problem have zero coefficients, i.e., $G = O$.

Computation details. While there are open-source packages available for solving a group lasso problem, they are still relatively slow when applied to large instance for practical usage. For example, given a specific value for the tuning parameter, λ , our experiments observed that, using the **gglasso** R package, we can not obtain a solution within five hours for typical instances with $p \sim 10^4$. Instead, we use Gurobi to solve the problem based on the SOCP formulation for the empirical group lasso. The formulation aligns with Equation 9 but omits the unbiasedness constraint.

4 Monte Carlo simulations

To evaluate the performance of various reconciliation methods with time series selection outlined in Section 3, we carry out two simulations with different designs. In both simulations, we consider a hierarchy comprising two levels of aggregation, as shown in Figure 1. Specifically, the structure has four time series at the bottom level, and seven time series in total, i.e., $n_b = 4$, and $n = 7$. In addition, the bottom-level series are first generated and then summed appropriately to obtain aggregated time series at higher levels.

In particular, Section 4.1 delves into a setup where the bottom-level series are generated using a structural time series model, but model misspecification exists for some series within the hierarchical structure. In Section 4.2, we explore the impact of correlation between series on the performance of reconciled forecasts.

4.1 Setup 1: Exploring the effect of model misspecification

In this simulation design, we follow a simulation setup similar to Wickramasuriya, Athanasopoulos & Hyndman (2019), assuming that the bottom-level time series are generated using the basic structural time series model

$$b_t = \mu_t + \gamma_t + \eta_t,$$

where μ_t , γ_t , and η_t are trend, seasonality, and error components, respectively. The trend and seasonality components are defined by

$$\begin{aligned}\mu_t &= \mu_{t-1} + v_t + \varrho_t, & \varrho_t &\sim \mathcal{N}(\mathbf{0}, \sigma_\varrho^2 \mathbf{I}_4), \\ v_t &= v_{t-1} + \zeta_t, & \zeta_t &\sim \mathcal{N}(\mathbf{0}, \sigma_\zeta^2 \mathbf{I}_4), \\ \gamma_t &= -\sum_{i=1}^{s-1} \gamma_{t-i} + \omega_t, & \omega_t &\sim \mathcal{N}(\mathbf{0}, \sigma_\omega^2 \mathbf{I}_4),\end{aligned}$$

where ϱ_t , ζ_t , and ω_t are error terms independent of each other and over time. The error term η_t is generated independently from an ARIMA($p, 0, q$) process, where p and q take values of 0 or 1 with equal probability. The coefficients for the AR and MA components in the ARIMA process are sampled randomly from a uniform distribution within the range $[0.5, 0.7]$, and the contemporaneous error covariance matrix is given by

$$\begin{bmatrix} 5 & 3 & 2 & 1 \\ 3 & 4 & 2 & 1 \\ 2 & 2 & 5 & 3 \\ 1 & 1 & 3 & 4 \end{bmatrix},$$

which enables correlations among time series in a hierarchical structure.

We set $s = 4$ for quarterly data with error variances $\sigma_\varrho^2 = 2$, $\sigma_\zeta^2 = 0.007$, and $\sigma_\omega^2 = 7$, respectively. The initial values for μ_0 , v_0 , γ_0 , γ_1 , and γ_2 are generated independently from a multivariate normal distribution with zero mean and identity covariance matrix. For each series at the bottom level, we generate a total of $T + h = 180$ observations, with the last $h = 16$ observations serving as the test set. Recall that the bottom-level series are aggregated to obtain the data for the aggregated levels. This process is repeated 500 times.

We use ETS models to generate base forecasts for all time series in the hierarchy, using the default settings as implemented in the **forecast** R package (Hyndman et al. 2023). To introduce model misspecification into our experiment, we deliberately undermine the quality of in-sample and out-of-sample forecasts (i.e., fitted values and base forecasts) for some specific time series. Specifically, we investigate three scenarios characterized by artificial model misspecification, where a 1.5 multiplier is applied to in-sample and out-of-sample forecasts for one series, i.e., series AA at the bottom level, series A at the middle level, and series Total at the top level, resulting in Scenario I, Scenario II, and Scenario III, respectively.

The results for Scenario I, II, and III are presented in Table 1, Table 2, and Table 3, respectively. Each table reports the average root mean squared error (RMSE) for each level as well as the whole structure (denoted as *Average*). The *Base* row shows the average RMSE of the base forecasts,

while entries below this row reporting the percentage decrease (negative) or increase (positive) in the average RMSE of the reconciled forecasts compared to the base forecasts.

Table 1: Out-of-sample forecast results for the simulated data in Scenario I (model misspecification introduced in series AA). “Base” shows the average RMSE of the base forecasts. Entries below this row indicate the percentage decrease (negative) or increase (positive) in the average RMSE of the reconciled forecasts compared to the base forecasts. The entries with the lowest values in each column are highlighted in blue. In each panel, methods that outperform the benchmark method are marked in bold.

| Method | Top | | | | Middle | | | | Bottom | | | | Average | | | |
|-----------------|-------------|-------------|------------|------------|-------------|-------------|-------------|------------|--------------|--------------|--------------|--------------|--------------|--------------|--------------|--------------|
| | h=1 | 1-4 | 1-8 | 1-16 | h=1 | 1-4 | 1-8 | 1-16 | h=1 | 1-4 | 1-8 | 1-16 | h=1 | 1-4 | 1-8 | 1-16 |
| Base | 9.6 | 10.7 | 12.6 | 15.6 | 6.3 | 7.3 | 8.6 | 10.8 | 6.4 | 7.5 | 8.3 | 9.8 | 6.8 | 7.9 | 9.0 | 10.9 |
| BU | 57.8 | 68.5 | 53.7 | 38.9 | 58.2 | 61.8 | 48.1 | 34.4 | 0.0 | 0.0 | 0.0 | 0.0 | 27.0 | 29.6 | 23.8 | 17.7 |
| OLS | 0.6 | 2.2 | 1.8 | 1.4 | 7.1 | 6.4 | 4.6 | 3.1 | -7.6 | -8.6 | -8.2 | -7.3 | -2.1 | -2.5 | -2.7 | -2.6 |
| OLS-subset | 0.6 | 1.8 | 1.5 | 1.3 | 7.2 | 5.2 | 3.8 | 2.6 | -8.3 | -12.9 | -11.6 | -9.9 | -2.4 | -5.2 | -4.8 | -4.1 |
| OLS-intuitive | 0.8 | 2.6 | 2.1 | 1.8 | 7.5 | 6.1 | 4.4 | 3.0 | -9.0 | -12.8 | -11.6 | -9.9 | -2.7 | -4.8 | -4.5 | -3.8 |
| OLS-lasso | 0.6 | 2.2 | 1.8 | 1.6 | 7.4 | 6.7 | 4.8 | 3.2 | -7.6 | -8.5 | -8.1 | -7.2 | -2.0 | -2.4 | -2.6 | -2.5 |
| WLSs | 7.3 | 10.6 | 8.1 | 5.9 | 15.6 | 16.0 | 11.8 | 8.0 | -6.9 | -7.8 | -7.4 | -6.4 | 1.9 | 2.0 | 1.0 | 0.2 |
| WLSs-subset | 5.0 | 5.7 | 4.6 | 3.6 | 12.3 | 10.0 | 7.5 | 5.2 | -7.6 | -10.5 | -9.6 | -8.2 | 0.2 | -2.0 | -2.1 | -2.0 |
| WLSs-intuitive | 7.1 | 9.2 | 7.1 | 5.2 | 16.5 | 15.5 | 11.5 | 7.9 | -6.8 | -9.2 | -8.4 | -7.3 | 2.1 | 0.9 | 0.1 | -0.4 |
| WLSs-lasso | 7.3 | 10.3 | 8.0 | 5.9 | 15.7 | 16.1 | 11.8 | 8.1 | -7.0 | -7.8 | -7.3 | -6.4 | 1.9 | 2.0 | 1.0 | 0.2 |
| WLSv | 1.0 | 2.9 | 2.3 | 1.9 | 4.5 | 4.3 | 3.2 | 2.1 | -25.8 | -26.4 | -22.7 | -18.3 | -12.4 | -12.6 | -10.7 | -8.4 |
| WLSv-subset | -1.0 | 0.3 | 0.4 | 0.5 | 0.6 | 0.6 | 0.5 | 0.3 | -32.3 | -32.2 | -27.3 | -21.7 | -17.3 | -17.3 | -14.2 | -10.9 |
| WLSv-intuitive | -0.5 | 0.2 | 0.3 | 0.5 | 0.9 | 0.7 | 0.5 | 0.3 | -32.3 | -32.3 | -27.4 | -21.7 | -17.1 | -17.3 | -14.2 | -10.9 |
| WLSv-lasso | 0.4 | 1.5 | 1.5 | 1.4 | 3.0 | 2.5 | 2.0 | 1.3 | -28.5 | -29.2 | -24.9 | -19.9 | -14.4 | -14.9 | -12.3 | -9.5 |
| MinT | -0.4 | 0.7 | 0.9 | 0.6 | 0.7 | 0.7 | 0.6 | 0.3 | -32.9 | -33.4 | -28.3 | -22.5 | -17.5 | -17.8 | -14.6 | -11.3 |
| MinT-subset | -0.6 | 0.7 | 0.8 | 0.7 | 0.6 | 0.8 | 0.6 | 0.3 | -33.0 | -33.1 | -28.0 | -22.3 | -17.6 | -17.6 | -14.5 | -11.2 |
| MinT-intuitive | -0.4 | 0.7 | 0.9 | 0.6 | 0.7 | 0.7 | 0.6 | 0.3 | -32.9 | -33.4 | -28.3 | -22.5 | -17.5 | -17.8 | -14.6 | -11.3 |
| MinT-lasso | -0.7 | 0.3 | 0.6 | 0.4 | 0.3 | 0.4 | 0.4 | 0.1 | -33.2 | -33.7 | -28.5 | -22.6 | -17.8 | -18.1 | -14.8 | -11.4 |
| MinTs | -0.9 | 0.6 | 0.7 | 0.5 | 0.6 | 0.6 | 0.5 | 0.2 | -32.9 | -33.5 | -28.3 | -22.5 | -17.6 | -17.9 | -14.6 | -11.3 |
| MinTs-subset | -0.7 | 0.9 | 1.1 | 1.0 | 0.7 | 0.8 | 0.7 | 0.4 | -33.0 | -33.1 | -27.9 | -22.2 | -17.6 | -17.5 | -14.3 | -11.0 |
| MinTs-intuitive | -0.9 | 0.6 | 0.7 | 0.5 | 0.6 | 0.6 | 0.5 | 0.2 | -32.9 | -33.5 | -28.3 | -22.5 | -17.6 | -17.9 | -14.6 | -11.3 |
| MinTs-lasso | -0.9 | 0.4 | 0.6 | 0.5 | 0.6 | 0.4 | 0.4 | 0.1 | -33.2 | -33.6 | -28.4 | -22.6 | -17.7 | -18.0 | -14.8 | -11.4 |
| EMinT | 2.2 | 2.9 | 2.5 | 1.7 | 2.5 | 2.9 | 2.3 | 1.3 | -31.9 | -32.3 | -27.5 | -22.0 | -15.9 | -16.2 | -13.4 | -10.5 |
| Elasso | 1.5 | 2.8 | 2.4 | 1.7 | 2.1 | 2.8 | 2.3 | 1.3 | -32.1 | -32.2 | -27.4 | -21.9 | -16.3 | -16.2 | -13.3 | -10.5 |

Focusing on the results of the benchmark reconciliation methods, we find that the bottom-up (BU) approach performs the best in both Scenario II and III but ranks as the worst overall in Scenario I. This is not surprising, as bottom-level base forecasts are deteriorated in Scenario I, while higher-level base forecasts are deteriorated in Scenario II and III. Moreover, the WLSv, MinT, and MinTs approaches perform especially well, benefiting from their ability to consider the in-sample covariance of base forecast errors, allowing for larger range of adjustments for reconciliation. EMinT also provides accurate reconciled forecasts in our setup, where the in-sample forecasts for specific series are intentionally undermined, a situation that can be detected by the in-sample information based EMinT method. However, OLS and WLSs perform much worse than other benchmark methods in this simulation setup.

In all three scenarios, our proposed methods consistently produce either improved or comparable reconciled forecasts compared to the benchmark methods. The improvements are

Table 2: Out-of-sample forecast results for the simulated data in Scenario II (model misspecification introduced in series A). “Base” shows the average RMSE of the base forecasts. Entries below this row indicate the percentage decrease (negative) or increase (positive) in the average RMSE of the reconciled forecasts compared to the base forecasts. The entries with the lowest values in each column are highlighted in blue. In each panel, methods that outperform the benchmark method are marked in bold.

| Method | Top | | | | Middle | | | | Bottom | | | | Average | | | |
|-----------------|-------------|------------|------------|------------|--------------|--------------|--------------|--------------|------------|------------|------------|------------|--------------|--------------|--------------|--------------|
| | h=1 | 1-4 | 1-8 | 1-16 | h=1 | 1-4 | 1-8 | 1-16 | h=1 | 1-4 | 1-8 | 1-16 | h=1 | 1-4 | 1-8 | 1-16 |
| Base | 9.6 | 10.7 | 12.6 | 15.6 | 12.1 | 14.4 | 15.3 | 17.0 | 4.2 | 4.9 | 5.9 | 7.5 | 7.2 | 8.5 | 9.6 | 11.4 |
| BU | -1.0 | 0.4 | 0.6 | 0.7 | -47.7 | -49.6 | -43.6 | -36.2 | 0.0 | 0.0 | 0.0 | 0.0 | -23.0 | -24.0 | -19.8 | -15.3 |
| OLS | 8.5 | 13.9 | 10.4 | 7.6 | -28.2 | -29.4 | -26.7 | -23.1 | 22.9 | 23.9 | 17.0 | 11.3 | -4.2 | -3.8 | -4.2 | -4.1 |
| OLS-subset | -0.5 | 0.5 | 0.6 | 0.7 | -46.3 | -49.0 | -43.2 | -35.9 | 2.2 | 1.0 | 0.7 | 0.5 | -21.5 | -23.4 | -19.4 | -15.0 |
| OLS-intuitive | -0.5 | 0.5 | 0.6 | 0.6 | -46.5 | -49.0 | -43.2 | -36.0 | 2.2 | 1.2 | 0.7 | 0.5 | -21.6 | -23.4 | -19.4 | -15.0 |
| OLS-lasso | -0.2 | 1.5 | 1.4 | 1.3 | -46.9 | -48.9 | -43.1 | -35.8 | 0.9 | 0.8 | 0.5 | 0.3 | -22.1 | -23.3 | -19.3 | -14.9 |
| WLSs | 12.1 | 18.6 | 14.0 | 10.2 | -34.4 | -35.1 | -31.7 | -26.9 | 15.6 | 17.0 | 12.0 | 8.0 | -9.0 | -8.0 | -7.6 | -6.5 |
| WLSs-subset | -0.1 | 1.2 | 1.1 | 1.1 | -46.7 | -48.8 | -43.1 | -35.8 | 1.5 | 1.1 | 0.8 | 0.6 | -21.8 | -23.2 | -19.2 | -14.8 |
| WLSs-intuitive | 0.0 | 1.2 | 1.0 | 0.9 | -46.5 | -48.8 | -43.1 | -35.9 | 1.7 | 1.3 | 0.9 | 0.6 | -21.6 | -23.1 | -19.2 | -14.9 |
| WLSs-lasso | -0.1 | 1.5 | 1.5 | 1.3 | -46.7 | -48.9 | -43.1 | -35.8 | 0.9 | 0.8 | 0.5 | 0.3 | -22.0 | -23.2 | -19.3 | -14.9 |
| WLSv | -0.8 | 2.3 | 1.8 | 1.6 | -46.3 | -47.9 | -42.3 | -35.2 | 1.6 | 1.9 | 1.2 | 0.8 | -21.7 | -22.2 | -18.6 | -14.4 |
| WLSv-subset | -0.7 | 1.3 | 1.4 | 1.4 | -46.9 | -48.7 | -42.9 | -35.6 | 1.0 | 1.0 | 0.8 | 0.6 | -22.2 | -23.1 | -19.1 | -14.7 |
| WLSv-intuitive | -0.4 | 1.5 | 1.4 | 1.2 | -46.9 | -48.6 | -42.8 | -35.6 | 0.9 | 1.2 | 0.9 | 0.7 | -22.2 | -23.0 | -19.0 | -14.7 |
| WLSv-lasso | -0.6 | 1.3 | 1.3 | 1.3 | -47.2 | -48.9 | -43.0 | -35.7 | 0.6 | 0.8 | 0.5 | 0.4 | -22.4 | -23.3 | -19.2 | -14.8 |
| MinT | 0.2 | 0.5 | 0.6 | 0.5 | -47.5 | -49.4 | -43.5 | -36.1 | 1.1 | 0.5 | 0.3 | 0.1 | -22.3 | -23.7 | -19.6 | -15.3 |
| MinT-subset | -0.1 | 0.8 | 0.9 | 0.9 | -46.9 | -49.1 | -43.3 | -36.0 | 1.7 | 0.9 | 0.5 | 0.3 | -21.9 | -23.4 | -19.4 | -15.1 |
| MinT-intuitive | 0.2 | 0.5 | 0.6 | 0.5 | -47.5 | -49.4 | -43.5 | -36.1 | 1.1 | 0.5 | 0.3 | 0.1 | -22.3 | -23.7 | -19.6 | -15.3 |
| MinT-lasso | -0.3 | 0.3 | 0.6 | 0.5 | -47.6 | -49.4 | -43.5 | -36.1 | 0.8 | 0.3 | 0.2 | 0.1 | -22.5 | -23.9 | -19.7 | -15.3 |
| MinTs | -0.3 | 0.3 | 0.4 | 0.4 | -47.6 | -49.5 | -43.6 | -36.2 | 0.7 | 0.2 | 0.1 | 0.0 | -22.6 | -23.9 | -19.8 | -15.3 |
| MinTs-subset | -0.8 | 0.5 | 0.8 | 0.8 | -47.2 | -49.2 | -43.4 | -36.0 | 1.0 | 0.7 | 0.4 | 0.3 | -22.3 | -23.6 | -19.5 | -15.1 |
| MinTs-intuitive | -0.3 | 0.3 | 0.4 | 0.4 | -47.6 | -49.5 | -43.6 | -36.2 | 0.7 | 0.2 | 0.1 | 0.0 | -22.6 | -23.9 | -19.8 | -15.3 |
| MinTs-lasso | -0.9 | 0.2 | 0.5 | 0.5 | -47.7 | -49.5 | -43.6 | -36.2 | 0.5 | 0.2 | 0.1 | 0.1 | -22.8 | -24.0 | -19.8 | -15.3 |
| EMinT | 2.2 | 2.9 | 2.5 | 1.7 | -46.2 | -48.1 | -42.4 | -35.3 | 3.6 | 2.9 | 2.0 | 1.1 | -20.5 | -21.9 | -18.2 | -14.3 |
| Elasso | 1.4 | 2.7 | 2.4 | 1.6 | -46.4 | -48.2 | -42.4 | -35.4 | 3.1 | 3.2 | 2.1 | 1.2 | -20.9 | -21.9 | -18.2 | -14.3 |

particularly pronounced when using OLS and WLSs estimators of W , which do not take into account the in-sample covariance of base forecast errors. One advantage of using the forecast reconciliation methods with selection proposed in this paper is that it reduces the difference introduced by using different estimates of W , thereby mitigating the risk of estimator selection. In some cases, such as Scenarios II and III, we can align the forecast accuracy achieved with different methods to match the best results we can obtain through time series selection in forecast reconciliation.

In addition, we report the proportion of time series being selected from the application of our proposed methods in 500 simulation instances, as shown in Table 4, Table 5, and Table 6 for each respective scenario. Clearly, our proposed methods select fewer time series from the hierarchy for forecast reconciliation, and generally improve forecast accuracy over the benchmark methods. Furthermore, we observe that the Subset method tends to return fewer time series compared to the Intuitive and Lasso methods, which aligns with our expectations. As discussed in Section 3, the Intuitive and Lasso methods tends to produce dense estimates.

Table 3: Out-of-sample forecast results for the simulated data in Scenario III (model misspecification introduced in series Total). “Base” shows the average RMSE of the base forecasts. Entries below this row indicate the percentage decrease (negative) or increase (positive) in the average RMSE of the reconciled forecasts compared to the base forecasts. The entries with the lowest values in each column are highlighted in blue. In each panel, methods that outperform the benchmark method are marked in bold.

| Method | Top | | | | Middle | | | | Bottom | | | | Average | | | |
|-----------------|--------------|--------------|--------------|--------------|-------------|-------------|-------------|-------------|-------------|-------------|-------------|-------------|--------------|--------------|--------------|--------------|
| | h=1 | 1-4 | 1-8 | 1-16 | h=1 | 1-4 | 1-8 | 1-16 | h=1 | 1-4 | 1-8 | 1-16 | h=1 | 1-4 | 1-8 | 1-16 |
| Base | 25.0 | 30.3 | 30.9 | 32.3 | 6.3 | 7.3 | 8.6 | 10.8 | 4.2 | 4.9 | 5.9 | 7.5 | 7.8 | 9.2 | 10.3 | 12.0 |
| BU | -62.0 | -64.4 | -59.0 | -51.5 | -0.3 | 0.0 | 0.1 | 0.0 | 0.0 | 0.0 | 0.0 | 0.0 | -28.5 | -30.2 | -25.3 | -19.8 |
| OLS | -34.8 | -35.5 | -33.5 | -30.1 | 45.3 | 50.6 | 37.7 | 25.1 | 27.7 | 29.9 | 21.2 | 13.7 | 3.1 | 3.8 | 1.6 | -0.2 |
| OLS-subset | -35.3 | -41.9 | -39.2 | -35.0 | 43.9 | 39.5 | 29.5 | 19.6 | 27.1 | 23.6 | 16.8 | 10.9 | 2.4 | -3.5 | -4.2 | -4.5 |
| OLS-intuitive | -41.2 | -49.2 | -45.5 | -40.0 | 35.1 | 26.8 | 20.3 | 13.7 | 21.9 | 15.9 | 11.5 | 7.6 | -4.0 | -12.2 | -10.9 | -9.1 |
| OLS-lasso | -61.8 | -63.6 | -58.1 | -50.9 | 0.4 | 1.3 | 1.3 | 0.7 | 0.3 | 0.8 | 0.6 | 0.4 | -28.2 | -29.3 | -24.5 | -19.2 |
| WLSs | -50.9 | -52.4 | -48.7 | -43.3 | 17.6 | 20.0 | 14.5 | 9.3 | 9.6 | 11.3 | 7.7 | 4.9 | -16.3 | -16.7 | -14.9 | -12.5 |
| WLSs-subset | -61.8 | -63.6 | -58.1 | -50.7 | 0.3 | 1.4 | 1.4 | 0.9 | 0.3 | 0.9 | 0.7 | 0.6 | -28.2 | -29.3 | -24.4 | -19.0 |
| WLSs-intuitive | -61.8 | -63.8 | -58.3 | -50.9 | 0.0 | 1.0 | 1.0 | 0.7 | 0.3 | 0.7 | 0.6 | 0.5 | -28.3 | -29.5 | -24.6 | -19.2 |
| WLSs-lasso | -61.7 | -63.5 | -58.0 | -50.7 | 0.5 | 1.5 | 1.4 | 0.9 | 0.3 | 0.9 | 0.7 | 0.5 | -28.1 | -29.2 | -24.4 | -19.1 |
| WLSv | -61.1 | -63.4 | -58.1 | -50.8 | 1.0 | 1.7 | 1.3 | 0.8 | 0.7 | 1.0 | 0.6 | 0.4 | -27.6 | -29.1 | -24.5 | -19.2 |
| WLSv-subset | -61.9 | -63.6 | -58.2 | -50.9 | 0.2 | 1.3 | 1.2 | 0.8 | 0.1 | 0.8 | 0.6 | 0.5 | -28.3 | -29.3 | -24.5 | -19.2 |
| WLSv-intuitive | -61.8 | -63.8 | -58.3 | -51.0 | 0.0 | 1.1 | 1.1 | 0.6 | 0.1 | 0.6 | 0.5 | 0.4 | -28.4 | -29.5 | -24.7 | -19.3 |
| WLSv-lasso | -61.8 | -63.9 | -58.4 | -51.1 | 0.2 | 0.9 | 0.9 | 0.5 | 0.1 | 0.5 | 0.4 | 0.3 | -28.3 | -29.6 | -24.8 | -19.4 |
| MinT | -62.1 | -64.3 | -58.9 | -51.6 | -0.2 | 0.6 | 0.5 | 0.2 | 0.8 | 0.5 | 0.3 | 0.1 | -28.3 | -29.9 | -25.1 | -19.8 |
| MinT-subset | -61.8 | -63.7 | -58.2 | -50.9 | 0.4 | 1.2 | 1.3 | 0.8 | 0.8 | 1.0 | 0.7 | 0.5 | -28.0 | -29.3 | -24.5 | -19.2 |
| MinT-intuitive | -62.1 | -64.3 | -58.9 | -51.6 | -0.2 | 0.6 | 0.5 | 0.2 | 0.8 | 0.5 | 0.3 | 0.1 | -28.3 | -29.9 | -25.1 | -19.8 |
| MinT-lasso | -62.1 | -64.4 | -58.9 | -51.5 | -0.3 | 0.3 | 0.4 | 0.1 | 0.6 | 0.3 | 0.1 | 0.1 | -28.4 | -30.1 | -25.2 | -19.8 |
| MinTs | -62.2 | -64.4 | -59.0 | -51.6 | -0.3 | 0.3 | 0.4 | 0.1 | 0.4 | 0.3 | 0.1 | 0.0 | -28.5 | -30.1 | -25.2 | -19.8 |
| MinTs-subset | -62.0 | -63.8 | -58.4 | -51.1 | 0.4 | 1.1 | 1.2 | 0.7 | 0.5 | 0.9 | 0.7 | 0.5 | -28.2 | -29.5 | -24.6 | -19.3 |
| MinTs-intuitive | -62.2 | -64.4 | -59.0 | -51.6 | -0.3 | 0.3 | 0.4 | 0.1 | 0.4 | 0.3 | 0.1 | 0.0 | -28.5 | -30.1 | -25.2 | -19.8 |
| MinTs-lasso | -62.2 | -64.4 | -58.9 | -51.5 | -0.2 | 0.3 | 0.4 | 0.1 | 0.2 | 0.2 | 0.1 | 0.0 | -28.5 | -30.1 | -25.2 | -19.8 |
| EMinT | -60.7 | -63.5 | -58.2 | -51.0 | 2.5 | 2.9 | 2.3 | 1.3 | 3.6 | 2.9 | 2.0 | 1.1 | -26.2 | -28.3 | -23.8 | -18.9 |
| Elasso | -60.9 | -63.6 | -58.2 | -51.1 | 2.3 | 2.8 | 2.3 | 1.3 | 3.1 | 3.1 | 2.1 | 1.2 | -26.5 | -28.3 | -23.8 | -18.9 |

4.2 Setup 2: Exploring the effect of correlation

We now consider to simulate a hierarchical structure with correlated series. A similar simulation to Wickramasuriya (2021) is implemented in this section. Using the same hierarchical structure as shown in Figure 1, we assume the data generating process for the time series at the bottom level follows a stationary first-order vector autoregressive model, i.e., VAR(1), given by

$$\mathbf{b}_t = \mathbf{c} + \begin{bmatrix} \mathbf{A}_1 & \mathbf{0} \\ \mathbf{0} & \mathbf{A}_2 \end{bmatrix} \mathbf{b}_{t-1} + \boldsymbol{\varepsilon}_t,$$

where \mathbf{c} is a constant vector with all entries set to 1, \mathbf{A}_1 and \mathbf{A}_2 are 2×2 matrices with eigenvalues $z_{1,2} = 0.6[\cos(\pi/3) \pm i \sin(\pi/3)]$ and $z_{3,4} = 0.9[\cos(\pi/6) \pm i \sin(\pi/6)]$, respectively, and $\boldsymbol{\varepsilon}_t \sim \mathcal{N}(\mathbf{0}, \boldsymbol{\Sigma})$, where

Table 4: Proportion of time series being selected after using the proposed reconciliation methods with selection in Scenario I. The last column displays a stacked barplot for each method, based on the total number of selected series data from 500 simulation instances, with a darker sub-bar indicating a larger number.

| | Top | A | B | AA | AB | BA | BB | Summary |
|-----------------|------|------|------|------|----|------|------|---------|
| OLS-subset | 0.52 | 0.79 | 0.57 | 0.79 | 1 | 0.91 | 0.85 | |
| OLS-intuitive | 0.80 | 0.90 | 0.81 | 0.80 | 1 | 0.85 | 0.86 | |
| OLS-lasso | 0.90 | 1.00 | 0.68 | 1.00 | 1 | 1.00 | 1.00 | |
| WLSs-subset | 0.85 | 0.91 | 0.86 | 0.90 | 1 | 0.97 | 0.97 | |
| WLSs-intuitive | 0.92 | 0.95 | 0.67 | 0.92 | 1 | 0.92 | 0.95 | |
| WLSs-lasso | 0.72 | 1.00 | 0.72 | 1.00 | 1 | 1.00 | 1.00 | |
| WLSv-subset | 0.50 | 0.62 | 0.42 | 0.19 | 1 | 0.81 | 0.87 | |
| WLSv-intuitive | 0.59 | 0.55 | 0.49 | 0.17 | 1 | 0.76 | 0.86 | |
| WLSv-lasso | 0.40 | 1.00 | 0.41 | 0.77 | 1 | 1.00 | 1.00 | |
| MinT-subset | 0.66 | 0.90 | 0.61 | 0.72 | 1 | 0.91 | 0.93 | |
| MinT-intuitive | 1.00 | 1.00 | 1.00 | 1.00 | 1 | 1.00 | 1.00 | |
| MinT-lasso | 0.80 | 0.96 | 0.84 | 0.72 | 1 | 0.98 | 0.97 | |
| MinTs-subset | 0.57 | 0.88 | 0.52 | 0.67 | 1 | 0.89 | 0.92 | |
| MinTs-intuitive | 1.00 | 1.00 | 1.00 | 1.00 | 1 | 1.00 | 1.00 | |
| MinTs-lasso | 0.68 | 1.00 | 0.66 | 0.74 | 1 | 1.00 | 1.00 | |
| Elasso | 0.82 | 0.63 | 0.69 | 1.00 | 1 | 1.00 | 1.00 | |

$$\Sigma = \begin{bmatrix} \Sigma_1 & 0 \\ 0 & \Sigma_2 \end{bmatrix}, \text{ and } \Sigma_1 = \Sigma_2 = \begin{bmatrix} 2 & \sqrt{6}\rho \\ \sqrt{6}\rho & 3 \end{bmatrix},$$

and $\rho \in \{0, \pm 0.2, \pm 0.4, \pm 0.6, \pm 0.8\}$ controls the error correlation in the simulated hierarchy.

For each time series at the bottom level, we generate a total of 101 observations, with the last one observation serving as the test set, i.e., $T = 100$ and $h = 1$. Once again, the data at the higher levels are obtained by aggregating the bottom-level series. The process is repeated 500 times for each candidate correlation, ρ .

For each series in the hierarchy, base forecasts are generated from ARMA models based on a training data comprising 100 observations. Specifically, we identify the best ARMA model with the minimum AICc (corrected Akaike information criterion) value for each series by using the automated algorithm implemented in the **forecast** R package. Additionally, when fitting ARMA models for time series Total, A, and BA, we introduce a slight bias by omitting the constant

Table 5: Proportion of time series being selected after using the proposed reconciliation methods with selection in Scenario II. The last column displays a stacked barplot for each method, based on the total number of selected series data from 500 simulation instances, with a darker sub-bar indicating a larger number.

| | Top | A | B | AA | AB | BA | BB | Summary |
|-----------------|------|------|------|------|------|------|------|---------|
| OLS-subset | 0.55 | 0.04 | 0.41 | 0.74 | 0.78 | 0.79 | 0.83 | |
| OLS-intuitive | 0.61 | 0.04 | 0.52 | 0.75 | 0.69 | 0.69 | 0.83 | |
| OLS-lasso | 0.04 | 0.35 | 0.02 | 1.00 | 1.00 | 1.00 | 1.00 | |
| WLSs-subset | 0.45 | 0.06 | 0.36 | 0.81 | 0.84 | 0.81 | 0.87 | |
| WLSs-intuitive | 0.61 | 0.06 | 0.48 | 0.75 | 0.71 | 0.73 | 0.84 | |
| WLSs-lasso | 0.02 | 0.33 | 0.02 | 1.00 | 1.00 | 1.00 | 1.00 | |
| WLSv-subset | 0.54 | 0.29 | 0.46 | 0.91 | 0.94 | 0.86 | 0.89 | |
| WLSv-intuitive | 0.59 | 0.32 | 0.53 | 0.82 | 0.86 | 0.77 | 0.86 | |
| WLSv-lasso | 0.27 | 0.42 | 0.26 | 1.00 | 1.00 | 1.00 | 1.00 | |
| MinT-subset | 0.69 | 0.64 | 0.66 | 0.95 | 0.96 | 0.90 | 0.90 | |
| MinT-intuitive | 1.00 | 1.00 | 1.00 | 1.00 | 1.00 | 1.00 | 1.00 | |
| MinT-lasso | 0.82 | 0.74 | 0.83 | 1.00 | 0.99 | 0.97 | 0.97 | |
| MinTs-subset | 0.62 | 0.63 | 0.58 | 0.95 | 0.96 | 0.90 | 0.86 | |
| MinTs-intuitive | 1.00 | 1.00 | 1.00 | 1.00 | 1.00 | 1.00 | 1.00 | |
| MinTs-lasso | 0.68 | 0.75 | 0.68 | 1.00 | 1.00 | 1.00 | 1.00 | |
| Elasso | 0.78 | 0.95 | 0.68 | 1.00 | 1.00 | 1.00 | 1.00 | |

term, which is a common scenario in practice. Figure 3 presents an illustrative example of a hierarchical time series generated. The left panels depict time plots for each series at different levels of structure, while right panels show the residuals obtained from forecasting each series using the ARMA model. Notably, despite our omission of the constant term when fitting ARMA models to the Total, A, and BA series, the residuals derived from the identified optimal ARMA models still exhibit fluctuations around zero and do not display significant deviations in comparison to the residuals from the other series. This is because the influence of the constant term is minimal in relation to the data variability. Thus, it may be challenging to identify the underperforming base forecasts of some series and exclude them from reconciliation.

Table 7 summarizes the average RMSE of the base forecasts across various error correlations and the percentage relative improvements in RMSE achieved by reconciliation methods relative to the base forecasts. The metrics are reported for each level and the whole structure.

Table 6: Proportion of time series being selected after using the proposed reconciliation methods with selection in Scenario III. The last column displays a stacked barplot for each method, based on the total number of selected series data from 500 simulation instances, with a darker sub-bar indicating a larger number.

| | Top | A | B | AA | AB | BA | BB | Summary |
|-----------------|------|------|------|------|------|------|------|---------|
| OLS-subset | 0.75 | 0.45 | 0.44 | 0.82 | 0.79 | 0.83 | 0.80 | |
| OLS-intuitive | 0.47 | 0.70 | 0.69 | 0.86 | 0.92 | 0.90 | 0.89 | |
| OLS-lasso | 0.38 | 0.01 | 0.01 | 1.00 | 1.00 | 1.00 | 1.00 | |
| WLSs-subset | 0.08 | 0.42 | 0.41 | 0.87 | 0.85 | 0.84 | 0.89 | |
| WLSs-intuitive | 0.06 | 0.55 | 0.50 | 0.66 | 0.87 | 0.69 | 0.88 | |
| WLSs-lasso | 0.35 | 0.03 | 0.03 | 1.00 | 1.00 | 1.00 | 1.00 | |
| WLSv-subset | 0.31 | 0.67 | 0.65 | 0.88 | 0.90 | 0.91 | 0.90 | |
| WLSv-intuitive | 0.34 | 0.63 | 0.60 | 0.80 | 0.89 | 0.84 | 0.87 | |
| WLSv-lasso | 0.45 | 0.35 | 0.36 | 1.00 | 1.00 | 1.00 | 1.00 | |
| MinT-subset | 0.69 | 0.78 | 0.80 | 0.91 | 0.91 | 0.91 | 0.91 | |
| MinT-intuitive | 1.00 | 1.00 | 1.00 | 1.00 | 1.00 | 1.00 | 1.00 | |
| MinT-lasso | 0.75 | 0.89 | 0.86 | 0.97 | 0.97 | 0.97 | 0.97 | |
| MinTs-subset | 0.67 | 0.74 | 0.76 | 0.90 | 0.89 | 0.88 | 0.91 | |
| MinTs-intuitive | 1.00 | 1.00 | 1.00 | 1.00 | 1.00 | 1.00 | 1.00 | |
| MinTs-lasso | 0.77 | 0.72 | 0.73 | 1.00 | 1.00 | 1.00 | 1.00 | |
| Elasso | 0.95 | 0.64 | 0.64 | 1.00 | 1.00 | 1.00 | 1.00 | |

The results show that, for OLS, WLSs, WLSv estimators, our proposed methods consistently dominate their respective benchmark methods at all levels when the error correlation is -0.8 . In general, as the error correlation ranges from -0.8 to 0.8 , the overall improvements in our methods over the benchmark methods show a slight decrease. Similar pattern is observed in the overall improvements of all benchmark reconciliation compared to the base forecasts. Of the methods we propose, the Subset methods display more consistently stable improvements overall. We should highlight the challenge of identifying the underperforming base forecasts in this simulation design, given that the omission of the constant term has minimal impact relative to the data variability. In addition, We observe that the MinT and MinTs methods perform especially well and our methods provide results on par with benchmark methods. This is attributed to the use of in-sample covariance by MinT and MinTs, which allows for large adjustments in reconciliation for base forecasts with high estimated error variance. Elasso forecasts are slightly worse than EMinT, possibly due to the difficulty of identifying underperforming base forecasts in this simulation setup.

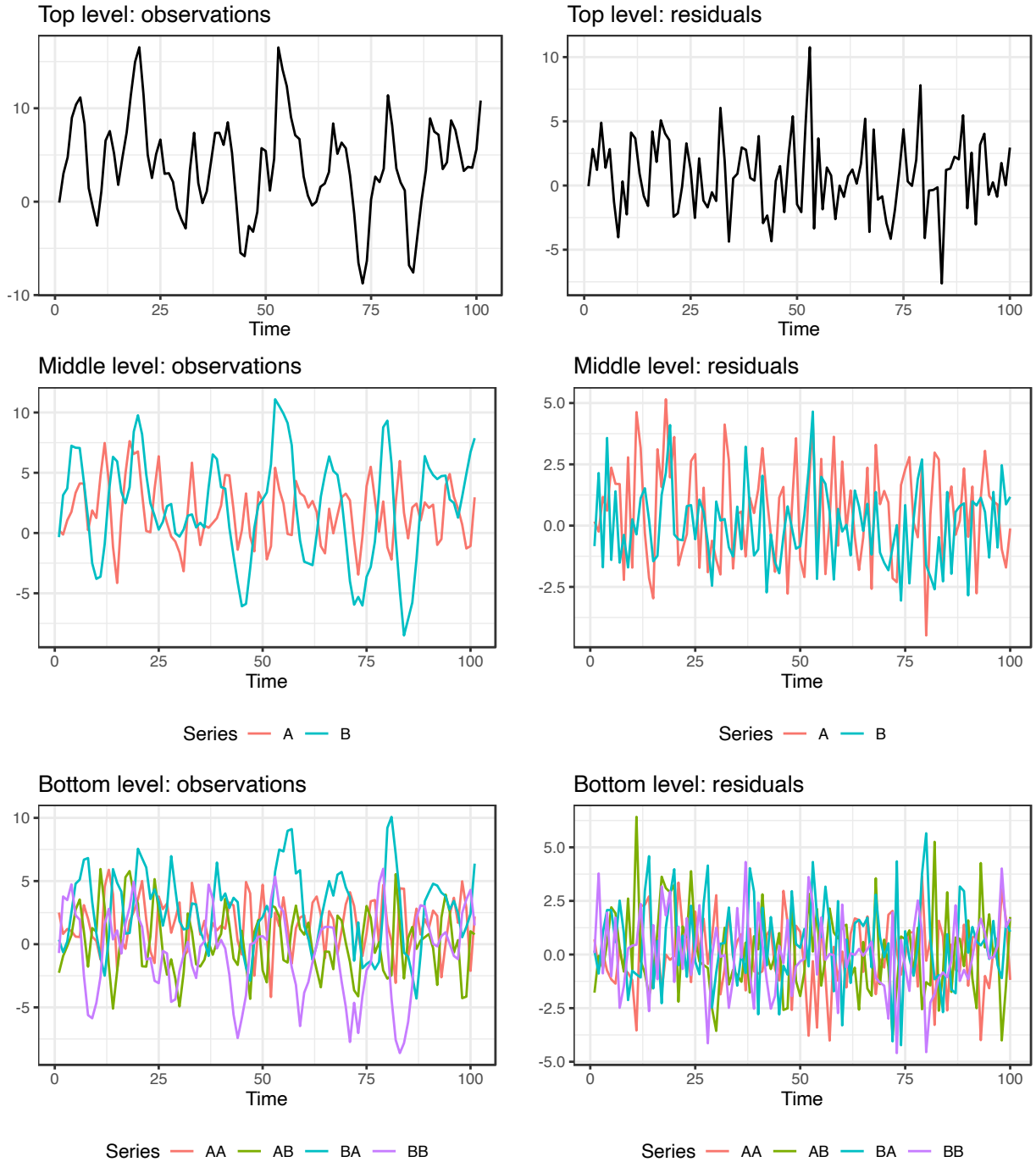


Figure 3: An example hierarchical time series and its in-sample residuals in Setup2.

We have also considered alternative error correlation values, $\rho = -0.6, -0.2, 0.2, 0.4$, for this simulation setting, but to save space, we do not present all results. The omitted results follow a similar pattern and are available upon request.

We present the proportion of time series being selected by applying our proposed methods in 500 simulation instances for error correlation coefficients of -0.8 and 0.8 in Table 8 and Table 9, respectively. One again, we note that it is difficult to exclude poor-performing base forecasts in this simulation design as the constant term omitted is very small compared to the data variability.

Table 7: Out-of-sample forecast results across various error correlations for the simulated data in Setup 2. “Base” shows the average RMSE of the base forecasts. Entries below this row indicate the percentage decrease (negative) or increase (positive) in the average RMSE of the reconciled forecasts compared to the base forecasts. The entries with the lowest values in each column are highlighted in blue. In each panel, methods that outperform the benchmark method are marked in bold.

| Method | Top | | | | | Middle | | | | | Bottom | | | | | Average | | | | |
|-----------------|--------------|--------------|--------------|--------------|--------------|--------------|--------------|-------------|-------------|-------------|-------------|-------------|-------------|-------------|-------------|--------------|--------------|-------------|-------------|-------------|
| | $\rho=-0.8$ | -0.4 | 0 | 0.4 | 0.8 | $\rho=-0.8$ | -0.4 | 0 | 0.4 | 0.8 | $\rho=-0.8$ | -0.4 | 0 | 0.4 | 0.8 | $\rho=-0.8$ | -0.4 | 0 | 0.4 | 0.8 |
| Base | 2.4 | 2.9 | 3.4 | 4.1 | 4.0 | 1.5 | 1.8 | 2.1 | 2.4 | 2.5 | 1.5 | 1.5 | 1.5 | 1.5 | 1.4 | 1.6 | 1.8 | 2.0 | 2.1 | 2.1 |
| BU | -17.0 | -9.0 | -6.7 | -7.0 | -7.4 | -6.8 | 0.4 | 4.8 | 5.7 | 2.8 | 0.0 | 0.0 | 0.0 | 0.0 | 0.0 | -5.3 | -1.9 | -0.2 | -0.1 | -1.0 |
| OLS | -11.0 | -8.2 | -7.7 | -8.2 | -8.0 | -3.5 | -0.7 | 3.1 | 2.5 | 0.8 | 0.7 | -0.6 | -2.0 | -2.3 | -2.1 | -2.8 | -2.4 | -1.8 | -2.4 | -2.7 |
| OLS-subset | -11.4 | -8.4 | -8.1 | -8.4 | -8.8 | -3.7 | -0.7 | 3.2 | 2.5 | 0.4 | 0.3 | -0.8 | -2.0 | -1.7 | -2.6 | -3.2 | -2.5 | -1.9 | -2.2 | -3.2 |
| OLS-intuitive | -11.6 | -8.0 | -7.8 | -8.0 | -8.4 | -3.6 | -0.4 | 3.7 | 2.5 | 0.3 | 0.6 | -0.2 | -1.3 | -0.4 | -1.5 | -3.0 | -2.0 | -1.3 | -1.6 | -2.8 |
| OLS-lasso | -19.2 | -9.8 | -7.2 | -8.7 | -8.2 | -10.5 | -1.7 | 2.9 | 2.4 | 0.8 | -0.8 | -0.8 | -1.6 | -2.3 | -2.1 | -7.1 | -3.1 | -1.6 | -2.5 | -2.8 |
| WLSs | -16.8 | -11.1 | -9.6 | -10.4 | -10.2 | -8.1 | -2.8 | 1.5 | 1.2 | -0.4 | -0.3 | -1.1 | -2.4 | -2.9 | -2.9 | -5.7 | -3.9 | -3.0 | -3.6 | -4.0 |
| WLSs-subset | -17.3 | -11.4 | -9.9 | -11.1 | -10.8 | -8.3 | -2.8 | 1.4 | 0.7 | -0.9 | -0.7 | -1.3 | -2.4 | -3.2 | -3.3 | -6.1 | -4.0 | -3.1 | -4.1 | -4.5 |
| WLSs-intuitive | -16.9 | -11.5 | -9.8 | -10.0 | -10.6 | -8.5 | -2.8 | 1.4 | 1.5 | -0.7 | -0.7 | -1.2 | -2.3 | -2.7 | -3.0 | -6.1 | -4.0 | -3.0 | -3.3 | -4.3 |
| WLSs-lasso | -18.3 | -11.1 | -9.2 | -10.5 | -9.8 | -9.3 | -2.4 | 1.4 | 1.2 | -0.1 | -0.8 | -1.0 | -2.4 | -2.9 | -2.8 | -6.6 | -3.7 | -2.9 | -3.7 | -3.7 |
| WLSv | -16.5 | -11.9 | -10.0 | -10.6 | -10.6 | -7.6 | -3.4 | 0.9 | 1.1 | -0.5 | -0.5 | -1.2 | -2.3 | -2.9 | -3.0 | -5.7 | -4.3 | -3.2 | -3.7 | -4.2 |
| WLSv-subset | -16.8 | -12.1 | -9.8 | -10.8 | -10.7 | -7.8 | -3.5 | 1.1 | 1.2 | -1.0 | -1.1 | -1.3 | -2.2 | -2.9 | -3.2 | -6.1 | -4.4 | -3.0 | -3.7 | -4.4 |
| WLSv-intuitive | -17.6 | -12.6 | -10.1 | -10.5 | -10.6 | -8.7 | -3.8 | 0.7 | 1.1 | -0.8 | -1.9 | -1.5 | -2.3 | -3.0 | -3.0 | -7.0 | -4.7 | -3.3 | -3.7 | -4.3 |
| WLSv-lasso | -19.8 | -11.6 | -9.7 | -10.5 | -10.6 | -10.5 | -3.0 | 1.2 | 1.2 | -0.5 | -1.2 | -1.1 | -2.2 | -2.9 | -3.0 | -7.5 | -4.1 | -3.0 | -3.7 | -4.2 |
| MinT | -25.4 | -18.8 | -12.4 | -15.3 | -12.6 | -15.5 | -7.0 | 0.0 | -2.0 | -2.0 | -4.0 | -4.6 | -4.3 | -5.8 | -5.1 | -11.4 | -8.5 | -5.0 | -7.2 | -6.0 |
| MinT-subset | -25.4 | -18.8 | -12.4 | -15.3 | -12.6 | -15.5 | -7.0 | 0.0 | -2.0 | -2.0 | -4.0 | -4.6 | -4.3 | -5.8 | -5.1 | -11.4 | -8.5 | -5.0 | -7.2 | -6.0 |
| MinT-intuitive | -25.4 | -18.8 | -12.4 | -15.3 | -12.6 | -15.5 | -7.0 | 0.0 | -2.0 | -2.0 | -4.0 | -4.6 | -4.3 | -5.8 | -5.1 | -11.4 | -8.5 | -5.0 | -7.2 | -6.0 |
| MinT-lasso | -25.4 | -18.8 | -12.4 | -15.3 | -12.6 | -15.5 | -7.0 | 0.0 | -2.0 | -2.0 | -4.0 | -4.6 | -4.3 | -5.8 | -5.1 | -11.4 | -8.5 | -5.0 | -7.2 | -6.0 |
| MinTs | -25.4 | -17.7 | -12.1 | -14.2 | -12.5 | -16.1 | -6.8 | -0.8 | -1.6 | -2.4 | -4.0 | -4.6 | -4.9 | -5.9 | -5.2 | -11.6 | -8.2 | -5.4 | -6.8 | -6.2 |
| MinTs-subset | -25.2 | -17.6 | -12.1 | -14.2 | -12.5 | -16.1 | -6.8 | -0.8 | -1.6 | -2.4 | -3.9 | -4.6 | -4.9 | -5.9 | -5.2 | -11.5 | -8.2 | -5.4 | -6.8 | -6.2 |
| MinTs-intuitive | -25.4 | -17.7 | -12.1 | -14.2 | -12.5 | -16.1 | -6.8 | -0.8 | -1.6 | -2.4 | -4.0 | -4.6 | -4.9 | -5.9 | -5.2 | -11.6 | -8.2 | -5.4 | -6.8 | -6.2 |
| MinTs-lasso | -25.4 | -17.6 | -12.1 | -14.2 | -12.5 | -16.1 | -6.7 | -0.8 | -1.6 | -2.4 | -4.0 | -4.6 | -4.9 | -5.9 | -5.2 | -11.6 | -8.2 | -5.4 | -6.8 | -6.2 |
| EMinT | -31.2 | -19.8 | -12.5 | -14.1 | -11.1 | -22.9 | -10.9 | -2.4 | -3.2 | -1.0 | -7.4 | -7.3 | -6.9 | -7.5 | -5.1 | -16.4 | -11.2 | -6.9 | -7.9 | -5.3 |
| Elasso | -31.0 | -19.1 | -11.1 | -13.6 | -11.2 | -22.7 | -9.7 | -1.8 | -2.4 | -1.7 | -7.4 | -7.2 | -6.1 | -5.7 | -3.5 | -16.3 | -10.6 | -6.0 | -6.8 | -4.9 |

As observed in Table 8, for the OLS, WLSs, and WLS estimators, the Subset and Intuitive methods are still able to exclude the series Total, A, and BA in some instances, in which small biases are introduced in model fitting, while essentially retaining the rest series in the hierarchy. The Subset methods perform superior to the Intuitive method in selection. The Lasso methods typically select all bottom-level series since they tend to yield dense estimates. When dealing with a high positive error correlation, Table 9 shows that it becomes somewhat challenging to identify and exclude the series that should be omitted in reconciliation. Hence, our methods are preferred, particularly when the error correlation within the hierarchical structure is negative.

5 Applications

In this section we perform two empirical applications to investigate the performance of our proposed methods and compare them with state-of-the-art reconciliation approaches. Section 5.1 considers Australian domestic tourism flows with a natural geographical hierarchy, while Section 5.2 focuses on a grouped hierarchy built using the Australian labour force survey data released by the Australian Bureau of Statistics.

Table 8: Proportion of time series being selected after using the proposed reconciliation methods with selection in Setup 2 with the error correlation being -0.8. The last column displays a stacked barplot for each method, based on the total number of selected series data from 500 simulation instances, with a darker sub-bar indicating a larger number.

| | Top | A | B | AA | AB | BA | BB | Summary |
|-----------------|------|------|------|------|----|------|------|---------|
| OLS-subset | 0.32 | 0.34 | 0.95 | 0.98 | 1 | 0.74 | 1.00 | |
| OLS-intuitive | 0.58 | 0.52 | 0.93 | 0.97 | 1 | 0.61 | 0.97 | |
| OLS-lasso | 0.61 | 0.34 | 0.38 | 1.00 | 1 | 1.00 | 1.00 | |
| WLSs-subset | 0.27 | 0.40 | 0.98 | 1.00 | 1 | 0.73 | 1.00 | |
| WLSs-intuitive | 0.49 | 0.57 | 0.96 | 1.00 | 1 | 0.74 | 0.99 | |
| WLSs-lasso | 0.48 | 0.62 | 0.72 | 1.00 | 1 | 1.00 | 1.00 | |
| WLSv-subset | 0.30 | 0.42 | 1.00 | 1.00 | 1 | 0.68 | 1.00 | |
| WLSv-intuitive | 0.49 | 0.53 | 0.99 | 1.00 | 1 | 0.47 | 1.00 | |
| WLSv-lasso | 0.35 | 0.70 | 0.85 | 1.00 | 1 | 1.00 | 1.00 | |
| MinT-subset | 1.00 | 1.00 | 1.00 | 1.00 | 1 | 1.00 | 1.00 | |
| MinT-intuitive | 1.00 | 1.00 | 1.00 | 1.00 | 1 | 1.00 | 1.00 | |
| MinT-lasso | 1.00 | 1.00 | 1.00 | 1.00 | 1 | 1.00 | 1.00 | |
| MinTs-subset | 0.87 | 0.85 | 1.00 | 1.00 | 1 | 0.85 | 1.00 | |
| MinTs-intuitive | 1.00 | 1.00 | 1.00 | 1.00 | 1 | 1.00 | 1.00 | |
| MinTs-lasso | 0.86 | 0.84 | 1.00 | 1.00 | 1 | 0.85 | 1.00 | |
| Elasso | 0.94 | 0.79 | 0.93 | 1.00 | 1 | 1.00 | 1.00 | |

5.1 Forecasting Australian domestic tourism

We consider Australian domestic tourism flows, measured as the number of overnight trips Australians spend away from home, and create a hierarchical structure using geographic divisions. The data are sourced from the National Visitor Survey and collected through computer-assisted telephone interviews involving approximately 120,000 Australian residents aged 15 years and older. The hierarchical structure starts with the national total tourism flow as the top-level aggregation, then disaggregates it into seven states and territories (referred to as *State* level hereafter), further divides them into 27 zones, and finally, into 76 regions, thus forming a natural geographical hierarchy.

Therefore, the hierarchy under consideration involves 76 monthly time series at the bottom level and 111 monthly series in total, i.e., $n_b = 76$ and $n = 111$. Each series in the hierarchy spans the period from January 1998 to December 2017, with a total of 240 observations.

Table 9: Proportion of time series being selected after using the proposed reconciliation methods with selection in Setup 2 with the error correlation being 0.8. The last column displays a stacked barplot for each method, based on the total number of selected series data from 500 simulation instances, with a darker sub-bar indicating a larger number.

| | Top | A | B | AA | AB | BA | BB | Summary |
|-----------------|------|------|------|------|------|------|------|---------|
| OLS-subset | 0.33 | 0.52 | 0.96 | 0.95 | 0.98 | 0.96 | 0.78 | |
| OLS-intuitive | 0.54 | 0.77 | 0.93 | 0.89 | 0.97 | 0.83 | 0.85 | |
| OLS-lasso | 0.69 | 0.53 | 0.60 | 1.00 | 1.00 | 1.00 | 1.00 | |
| WLSs-subset | 0.29 | 0.60 | 1.00 | 1.00 | 1.00 | 0.98 | 0.86 | |
| WLSs-intuitive | 0.63 | 0.67 | 0.99 | 0.98 | 1.00 | 0.93 | 0.86 | |
| WLSs-lasso | 0.69 | 0.76 | 0.91 | 1.00 | 1.00 | 1.00 | 1.00 | |
| WLSv-subset | 0.32 | 0.55 | 1.00 | 1.00 | 1.00 | 0.99 | 0.76 | |
| WLSv-intuitive | 0.58 | 0.56 | 1.00 | 1.00 | 0.98 | 1.00 | 0.75 | |
| WLSv-lasso | 0.77 | 0.84 | 0.99 | 1.00 | 1.00 | 1.00 | 1.00 | |
| MinT-subset | 1.00 | 1.00 | 1.00 | 1.00 | 1.00 | 1.00 | 1.00 | |
| MinT-intuitive | 1.00 | 1.00 | 1.00 | 1.00 | 1.00 | 1.00 | 1.00 | |
| MinT-lasso | 1.00 | 1.00 | 1.00 | 1.00 | 1.00 | 1.00 | 1.00 | |
| MinTs-subset | 1.00 | 1.00 | 1.00 | 1.00 | 1.00 | 1.00 | 1.00 | |
| MinTs-intuitive | 1.00 | 1.00 | 1.00 | 1.00 | 1.00 | 1.00 | 1.00 | |
| MinTs-lasso | 1.00 | 1.00 | 1.00 | 1.00 | 1.00 | 1.00 | 1.00 | |
| Elasso | 0.73 | 0.65 | 0.98 | 0.98 | 0.86 | 1.00 | 0.99 | |

Figure 4 shows the aggregate tourism flows for Australia as well as individual states, revealing pronounced seasonal patterns across the national total and states, albeit with varying seasonal patterns among the series. Notably, there was a significant growth starting from around 2010 for the national total flow and some states such as NSW (New South Wales), VIC (Victoria), QLD (Queensland), and WA (Western Australia). While flows are relatively flat for SA (South Australia), TAS (Tasmania), and NT (Northern Territory). Moreover, the time plot displays that there was a large decrease in tourism flows for WA occurred in 2016.

Our objective is to forecast tourism flows for each series in the geographical hierarchy while ensuring the coherence of forecasts across all levels. We split the data into a training set comprising 228 observations and test set with 12 observations, i.e., $T = 228$ and $h = 12$. To generate base forecasts, we select an optimal ETS model for each series using the automatic algorithm implemented in the **forecast** package for R. The base forecasts are then reconciled using our proposed methods and some state-of-the-art reconciliation methods.

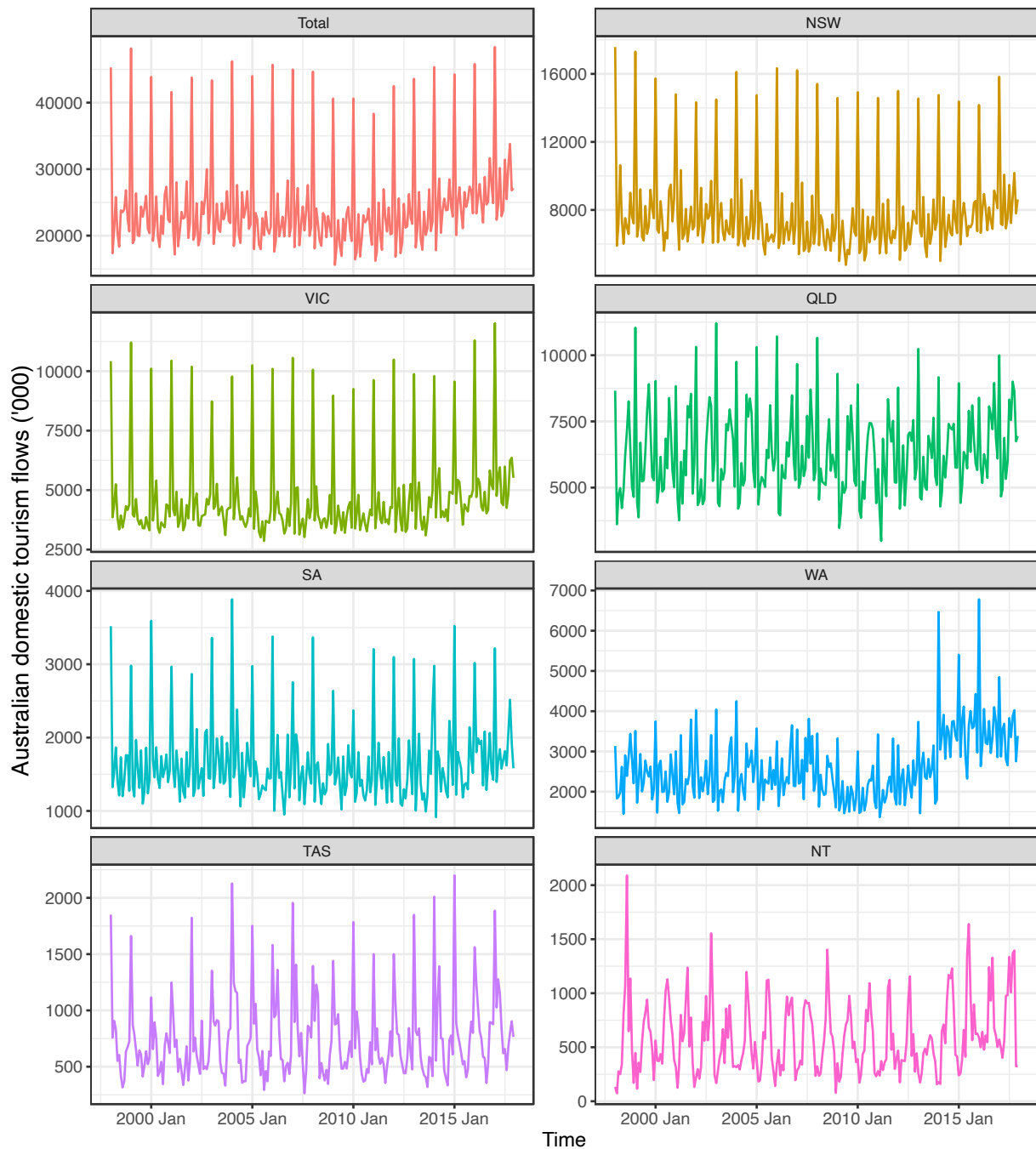


Figure 4: Domestic tourism flows from January 1998 to December 2017 for the whole of Australia as well as the states.

Table 10 reports the RMSE values for base forecasts generated by ETS models, along with the percentage relative improvements in average RMSE obtained by a particular reconciliation method relative to the base forecasts. We also show the reconciliation errors across each of the 111 series across the four levels in the hierarchy in Figure 5. The results show that, in the tourism application, the OLS method stands out as a strong performer when comparing to other benchmark methods such as WLSv and MinTs, which account for the in-sample covariance of base forecast errors. This highlights the effectiveness of the OLS method despite its simplicity.

Overall, all Subset methods with different estimators of G , i.e., OLS-subset, WLSs-subset, WLSv-subset, and MinTs-subset, give the same level of accuracy as their respective benchmark methods for one-step ahead forecasts, while showing gains for longer forecast horizons. The Intuitive and Lasso methods produce results identical to the corresponding benchmark methods, which is not surprising as ETS models typically do not yield extremely poor forecasts, making them challenging to be selected out using methods that tend to return dense estimates. When we relax the unbiasedness constraint, EMinT is the worst performing method across all levels. This is attributed to its assumption that the series in the hierarchy are jointly weakly stationary, which is evidently not the case in the tourism application. The Elasso method presents significant improvement compared to the EMinT method, and it also outperforms other methods across almost all levels except for the bottom level.

Table 10: Out-of-sample forecast results for Australian domestic tourism data. “Base” shows the average RMSE of the base forecasts, while entries below this row indicate the percentage decrease (negative) or increase (positive) in the average RMSE of the reconciled forecasts compared to the base forecasts. The entries with the lowest values in each column are highlighted in blue. In each panel, methods that outperform the benchmark method are marked in bold.

| Method | Top | | | | State | | | | Zone | | | | Region | | | | Average | | | |
|-----------------|--------------|--------------|--------------|--------------|--------------|--------------|-------------|--------------|--------------|-------------|-------------|--------------|-------------|-------------|-------------|-------------|--------------|-------------|-------------|-------------|
| | h=1 | 1-4 | 1-8 | 1-12 | h=1 | 1-4 | 1-8 | 1-12 | h=1 | 1-4 | 1-8 | 1-12 | h=1 | 1-4 | 1-8 | 1-12 | h=1 | 1-4 | 1-8 | 1-12 |
| Base | 1158.2 | 716.6 | 1279.5 | 1907.6 | 452.7 | 323.3 | 349.9 | 424.8 | 165.5 | 163.6 | 160.7 | 179.7 | 100.8 | 89.4 | 88.2 | 94.1 | 148.3 | 127.9 | 133.1 | 152.1 |
| BU | 89.1 | 132.8 | 53.4 | 42.0 | -4.6 | 10.3 | 17.0 | 19.7 | 1.1 | -2.4 | 0.4 | 1.0 | 0.0 | 0.0 | 0.0 | 0.0 | 5.7 | 7.6 | 7.6 | 8.5 |
| OLS | -4.7 | -0.4 | 0.5 | 1.4 | -3.0 | -3.9 | -1.6 | -1.5 | -2.1 | -4.2 | -5.6 | -7.5 | 1.0 | -0.4 | -1.9 | -3.2 | -1.0 | -2.1 | -2.7 | -3.6 |
| OLS-subset | -4.7 | 8.0 | -1.4 | -14.1 | -3.0 | 5.5 | 0.3 | -7.9 | -2.1 | -1.5 | -3.7 | -8.7 | 1.0 | 1.7 | -0.1 | -2.3 | -1.0 | 1.7 | -1.2 | -6.5 |
| OLS-intuitive | -4.7 | -0.4 | 0.5 | 1.4 | -3.0 | -3.9 | -1.6 | -1.5 | -2.1 | -4.2 | -5.6 | -7.5 | 1.0 | -0.4 | -1.9 | -3.2 | -1.0 | -2.1 | -2.7 | -3.6 |
| OLS-lasso | -4.7 | -0.4 | 0.5 | 1.4 | -3.0 | -3.9 | -1.6 | -1.5 | -2.1 | -4.2 | -5.6 | -7.5 | 1.0 | -0.4 | -1.9 | -3.2 | -1.0 | -2.1 | -2.7 | -3.6 |
| WLSs | 25.1 | 55.2 | 20.8 | 19.1 | -15.8 | -5.0 | 3.5 | 6.2 | -5.9 | -5.4 | -4.7 | -5.0 | -0.2 | -0.8 | -1.6 | -2.2 | -3.0 | -0.1 | 0.3 | 0.9 |
| WLSs-subset | 25.1 | 18.7 | 0.8 | -7.8 | -15.8 | -2.7 | -2.1 | -6.2 | -5.9 | -4.1 | -4.8 | -8.5 | -0.2 | 0.3 | -1.0 | -2.5 | -3.0 | -0.6 | -2.1 | -5.5 |
| WLSs-intuitive | 25.1 | 55.2 | 20.8 | 19.1 | -15.8 | -5.0 | 3.5 | 6.2 | -5.9 | -5.4 | -4.7 | -5.0 | -0.2 | -0.8 | -1.6 | -2.2 | -3.0 | -0.1 | 0.3 | 0.9 |
| WLSs-lasso | 25.1 | 55.2 | 20.8 | 19.1 | -15.8 | -5.0 | 3.5 | 6.2 | -5.9 | -5.4 | -4.7 | -5.0 | -0.2 | -0.8 | -1.6 | -2.2 | -3.0 | -0.1 | 0.3 | 0.9 |
| WLSv | 38.2 | 76.2 | 29.6 | 25.6 | -17.4 | -3.1 | 7.0 | 9.9 | -5.0 | -4.3 | -3.1 | -3.2 | -4.2 | -1.6 | -1.8 | -2.1 | -3.9 | 1.3 | 2.0 | 2.8 |
| WLSv-subset | 38.2 | 34.5 | 10.7 | 8.5 | -17.4 | -8.8 | -0.8 | 1.4 | -5.0 | -5.5 | -5.3 | -6.7 | -4.1 | -2.0 | -2.6 | -3.4 | -3.9 | -2.3 | -2.0 | -2.2 |
| WLSv-intuitive | 38.2 | 76.2 | 29.6 | 25.6 | -17.4 | -3.1 | 7.0 | 9.9 | -5.0 | -4.3 | -3.1 | -3.2 | -4.2 | -1.6 | -1.8 | -2.1 | -3.9 | 1.3 | 2.0 | 2.8 |
| WLSv-lasso | 38.2 | 76.2 | 29.6 | 25.6 | -17.4 | -3.1 | 7.0 | 9.9 | -5.0 | -4.3 | -3.1 | -3.2 | -4.2 | -1.6 | -1.8 | -2.1 | -3.9 | 1.3 | 2.0 | 2.8 |
| MinTs | 20.6 | 53.6 | 21.6 | 19.0 | -22.2 | -7.2 | 3.5 | 6.3 | -12.1 | -6.6 | -5.1 | -5.3 | -5.3 | -2.6 | -2.8 | -3.1 | -8.6 | -1.8 | -0.3 | 0.4 |
| MinTs-subset | 20.6 | 20.0 | 6.4 | 5.6 | -22.2 | -11.3 | -2.5 | -0.1 | -12.1 | -7.5 | -6.4 | -7.8 | -5.3 | -2.9 | -3.2 | -3.9 | -8.6 | -4.5 | -3.2 | -3.3 |
| MinTs-intuitive | 20.6 | 53.6 | 21.6 | 19.0 | -22.2 | -7.2 | 3.5 | 6.3 | -12.1 | -6.6 | -5.1 | -5.3 | -5.3 | -2.6 | -2.8 | -3.1 | -8.6 | -1.8 | -0.3 | 0.4 |
| MinTs-lasso | 20.6 | 53.6 | 21.6 | 19.0 | -22.2 | -7.2 | 3.5 | 6.3 | -12.1 | -6.6 | -5.1 | -5.3 | -5.3 | -2.6 | -2.8 | -3.1 | -8.6 | -1.8 | -0.3 | 0.4 |
| EMinT | 116.5 | 97.8 | -15.8 | -13.7 | 149.4 | 114.5 | 63.5 | 47.5 | 108.4 | 68.4 | 60.6 | 54.2 | 122.1 | 103.1 | 90.2 | 78.2 | 123.2 | 93.9 | 67.9 | 55.5 |
| Elasso | -84.5 | -50.4 | -16.3 | -16.4 | -18.3 | 0.6 | -9.0 | -11.4 | -7.8 | -8.8 | -7.5 | -10.4 | 2.9 | 1.6 | 4.1 | 0.3 | -10.2 | -4.4 | -3.2 | -6.7 |

Table 11 presents a summary of the number of series selected using different proposed methods for each level as well as the optimal tuning parameter values identified. Here we only give the results of the Subset and Elasso methods since they are useful in the tourism application. Note that the variation in the scale of the optimal parameters for different methods comes from the difference in the scales of objective. We observe that the OLS-subset and WLSs-subset methods exclude some series at the State and Zone levels for forecast reconciliation. In contrast, the WLSv and MinTs methods retain all series, which is reasonable because they take into account the in-sample covariance, making themselves allow for larger adjustments made to series with large in-sample forecast error variances in forecast reconciliation. Nonetheless, the WLSv and MinTs

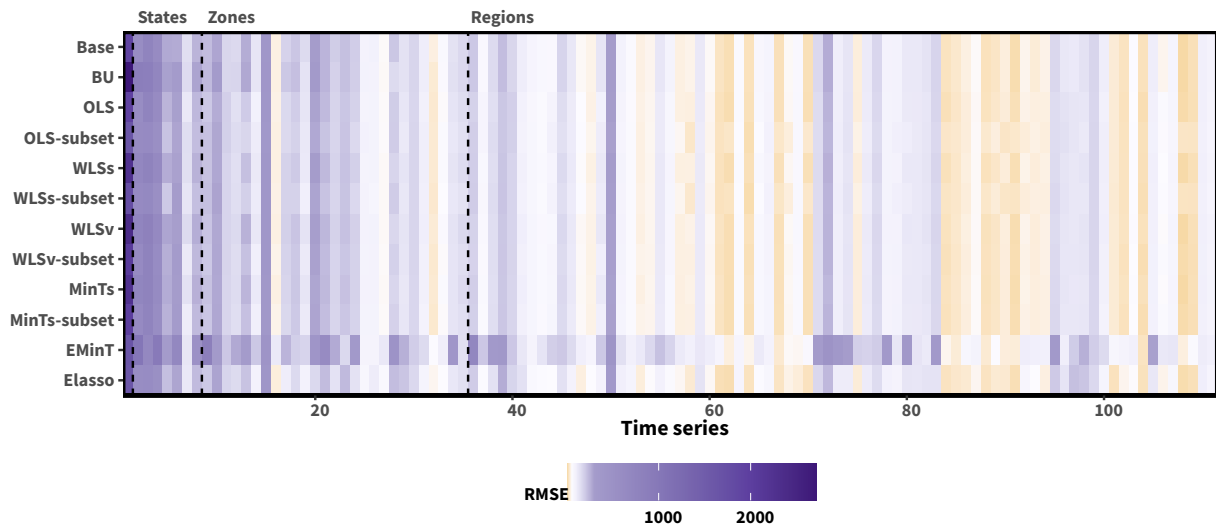


Figure 5: Average out-of-sample forecasting performance, measured in terms of RMSE (from 1- to 12-step-ahead), for each series across different reconciliation methods. Time series are arranged along the horizontal axis.

methods can still enhance the quality of reconciled forecasts due to the inclusion of shrinkage through additional ridge regularization. It is surprising that Elasso performs exceptionally well despite using only 13 series for reconciliation.

Table 11: Number of time series selected using different proposed methods and the optimal parameter values identified in the tourism application.

| | Number of time series retained | | | | | Optimal parameters | | |
|--------------|--------------------------------|-------|------|--------|-------|--------------------|-------------|-------------|
| | Top | State | Zone | Region | Total | λ | λ_0 | λ_2 |
| None | 1 | 7 | 27 | 76 | 111 | - | - | - |
| OLS-subset | 1 | 2 | 13 | 76 | 92 | - | 27.98 | 10.00 |
| WLSs-subset | 1 | 1 | 15 | 76 | 93 | - | 18.73 | 10.00 |
| WLSv-subset | 1 | 7 | 27 | 76 | 111 | - | 0.03 | 0.01 |
| MinTs-subset | 1 | 7 | 27 | 76 | 111 | - | 0.05 | 0.01 |
| Elasso | 1 | 4 | 0 | 8 | 13 | 71759.21 | - | - |

5.2 Forecasting Australian labour force

This section evaluates the performance of the proposed methods using a grouped hierarchy built using the Australian labour force dataset. The dataset from the Labour Force Survey are released by the Australian Bureau of Statistics, consisting of monthly data on the number of unemployed persons in Australia for the period from January 2010 to July 2023².

²The Labour Force Survey data is publicly available at <https://www.abs.gov.au/statistics/labour/employment-and-unemployment/labour-force-australia-detailed/aug-2023>.

There are a few missing values in the Australian labour force data. To deal with the missing observations, we use a random walk to give linear interpolation between points.

We construct a grouped hierarchy by disaggregating the number of unemployed persons over two independent attributes, duration of job search (referred to as *Duration* level), and State and Territory (referred to as *STT* level). The two attributes are crossed, but none are nested within the others. At the bottom level, the data are disaggregated by both attributes. We refer to the bottom level as *Duration* \times *STT* level. Specifically, there are six different groups of job search duration, under 1 month, 1-3 months, 3-6 months, 6-12 months, 1-2 years, and 2 years and over. Additionally, the number of unemployed persons in Australia can be disaggregated by eight states and territories, NSW, VIC, QLD, SA, WA, TAS, NT, ACT (Australian Capital Territory). So the final grouped hierarchy consists of the top series, 6 series at the *Duration* level, 8 series at the *STT* level, 48 series at the *Duration* \times *STT* level, giving 63 time series in total, each of length 163 observations.

The top panel in Figure 6 shows the total number of unemployed persons in Australia from January 2010 to July 2023, representing the top-level series in the grouped hierarchical structure. The monthly series shows strong seasonality within each year, marked by large peaks occurring every February. In addition, lower peaks occur in July, August, September, and October. There was a substantial increase in the number of unemployed persons during April, May, June, July of 2020, followed by a subsequent downward trend. The bottom-left panel displays the breakdown of unemployed individuals by state and territory, while the bottom-right panel presents the breakdown by the duration of job search. The plots display diverse and rich dynamics both within and between different levels of hierarchy. For example, there was noticeable growth observed during 2020 for some states such as NSW, VIC, and QLD, whereas other states did not experience such significant growth. Additionally, there is a resemblance in the seasonal patterns between NSW and QLD, while the seasonal pattern in VIC appears relatively heterogeneous. When comparing the series at the *STT* level and *Duration* level, we notice that the seasonal patterns in the *Duration* level series is more consistent and potentially easier to forecast.

For each series in the grouped hierarchy, we use the data spanning from January 2010 to July 2022 as the training set to select an optimal ETS model with the automatic algorithm implemented in the **forecast** package for R. Using these fitted ETS models, base forecasts are generated for $h = 1$ to 12-steps ahead. Subsequently, these base forecasts are used to perform forecast reconciliation, using the proposed methods and other state-of-the-art reconciliation approaches.

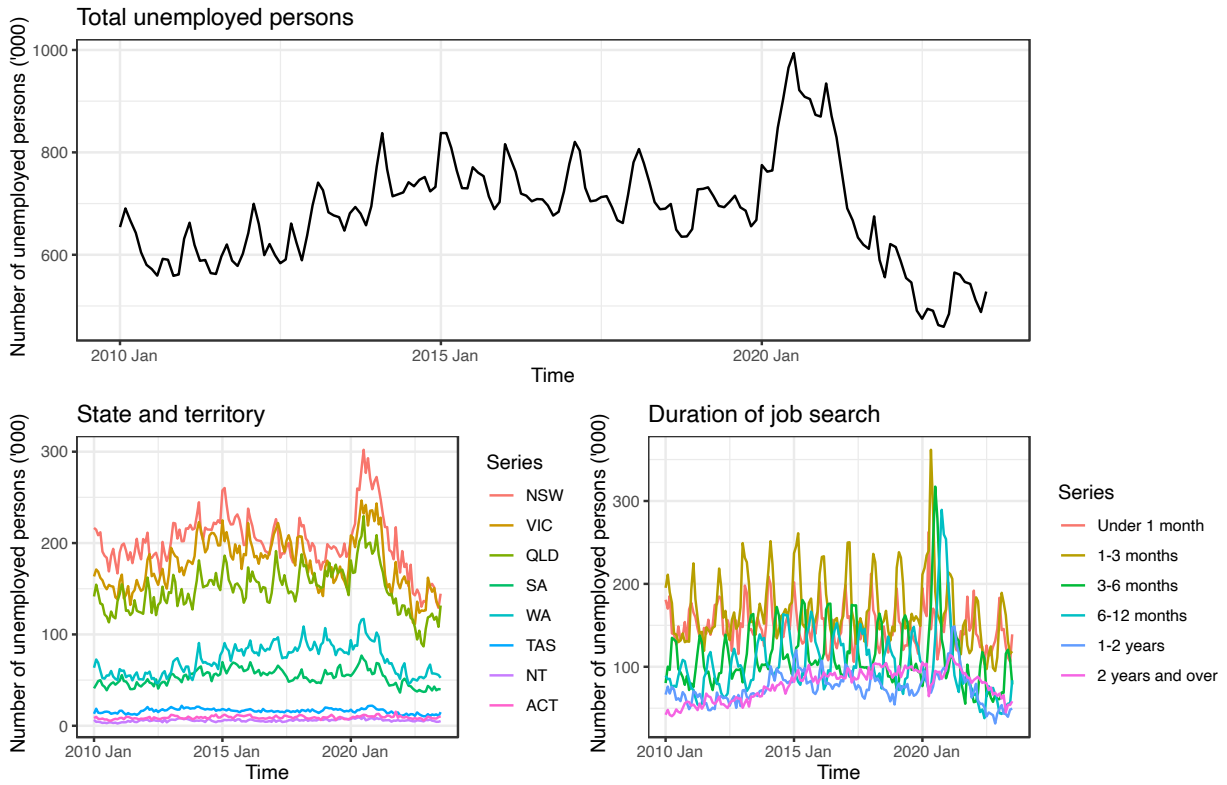


Figure 6: *Australia unemployed persons, disaggregated by state and territory, and by duration of job search.*

Table 12 presents the RMSE values for base forecasts generated by ETS models, as well as the percentage relative improvements obtained by each reconciliation method compared to the base forecasts. The results indicate that all Subset methods using different estimators of G , i.e., OLS-subset, WLSs-subset, WLSv-subset, and MinTs-subset, produce improved or comparable reconciled forecasts compared to their respective benchmark methods. The improvements in forecast accuracy become more noticeable for longer forecast horizons. Similar to the tourism application results, the Intuitive and Lasso methods yield results identical to the corresponding benchmark methods. This is because they tend to provide dense estimates, and ETS models typically do not result in extremely poor forecasts. The only exception is OLS-intuitive, which shows improved forecast accuracy at the top level but deterioration at other levels. Surprisingly, considering relaxing the unbiasedness constraint, the Elasso method demonstrates significant improvement compared to the EMinT method, and outperforms other methods across almost all levels except for the top level.

We provide the number of series selected at each level and the optimal tuning parameter values obtained using different proposed methods, as shown in Table 13. Here, we only showcase results from the Subset and Elasso methods, as they prove to be valuable in the labour force application. The results show that all Subset methods exclude some series when performing

Table 12: Out-of-sample forecast results for Australian labour force data. “Base” shows the average RMSE of the base forecasts, while entries below this row indicate the percentage decrease (negative) or increase (positive) in the average RMSE of the reconciled forecasts compared to the base forecasts. The entries with the lowest values in each column are highlighted in blue. In each panel, methods that outperform the benchmark method are marked in bold.

| Method | Top | | | | Duration | | | | STT | | | | Duration x STT | | | | Average | | | |
|-----------------|--------------|--------------|--------------|--------------|--------------|-------------|--------------|--------------|--------------|--------------|--------------|--------------|----------------|-------------|-------------|-------------|--------------|-------------|--------------|--------------|
| | h=1 | 1-4 | 1-8 | 1-12 | h=1 | 1-4 | 1-8 | 1-12 | h=1 | 1-4 | 1-8 | 1-12 | h=1 | 1-4 | 1-8 | 1-12 | h=1 | 1-4 | 1-8 | 1-12 |
| Base | 18.5 | 13.6 | 18.3 | 28.3 | 11.8 | 12.7 | 13.9 | 16.9 | 6.7 | 6.0 | 6.0 | 6.3 | 2.3 | 2.6 | 2.7 | 2.9 | 4.1 | 4.1 | 4.4 | 5.1 |
| BU | -81.5 | 33.4 | -19.9 | -45.0 | -30.7 | -9.2 | -7.9 | -10.1 | -12.9 | -10.4 | -13.4 | -13.5 | 0.0 | 0.0 | 0.0 | 0.0 | -17.1 | -2.8 | -5.9 | -9.3 |
| OLS | -16.2 | -14.2 | -13.4 | -10.4 | 2.5 | -2.6 | -2.7 | -0.6 | -1.8 | -0.9 | -1.9 | 0.3 | 6.7 | 5.1 | 5.1 | 4.9 | 2.1 | 0.7 | 0.4 | 1.1 |
| OLS-subset | -17.0 | -2.1 | -31.2 | -38.4 | 2.0 | -1.7 | -5.0 | -2.7 | -2.7 | -4.2 | -8.6 | -7.3 | 6.7 | 5.2 | 3.3 | 3.7 | 1.7 | 1.1 | -3.5 | -3.8 |
| OLS-intuitive | -79.6 | -23.9 | -31.9 | -32.1 | -13.0 | 0.4 | -0.8 | 0.3 | -8.9 | 4.9 | 7.0 | 13.2 | 6.3 | 12.3 | 12.4 | 11.6 | -8.5 | 5.6 | 4.7 | 4.4 |
| OLS-lasso | -16.2 | -14.2 | -13.4 | -10.4 | 2.5 | -2.6 | -2.7 | -0.6 | -1.8 | -0.9 | -1.9 | 0.3 | 6.7 | 5.1 | 5.1 | 4.9 | 2.1 | 0.7 | 0.4 | 1.1 |
| WLSs | -60.6 | -29.4 | -44.0 | -38.6 | -12.0 | -7.6 | -6.9 | -5.9 | -6.5 | -8.1 | -9.4 | -8.0 | 3.2 | 1.7 | 1.7 | 1.6 | -7.7 | -4.4 | -5.8 | -5.9 |
| WLSs-subset | -61.6 | -22.4 | -47.3 | -50.4 | -12.0 | -8.0 | -10.5 | -7.8 | -6.6 | -10.7 | -14.3 | -12.8 | 3.2 | 5.6 | 4.1 | 5.9 | -7.8 | -2.8 | -6.7 | -6.4 |
| WLSs-intuitive | -60.6 | -29.4 | -44.0 | -38.6 | -12.0 | -7.6 | -6.9 | -5.9 | -6.5 | -8.1 | -9.4 | -8.0 | 3.2 | 1.7 | 1.7 | 1.6 | -7.7 | -4.4 | -5.8 | -5.9 |
| WLSs-lasso | -60.6 | -29.4 | -44.0 | -38.6 | -12.0 | -7.6 | -6.9 | -5.9 | -6.5 | -8.1 | -9.4 | -8.0 | 3.2 | 1.7 | 1.7 | 1.6 | -7.7 | -4.4 | -5.8 | -5.9 |
| WLSv | -60.6 | -29.1 | -41.4 | -36.6 | -14.5 | -8.7 | -5.6 | -4.8 | -3.3 | -6.8 | -8.0 | -7.0 | 5.5 | 2.6 | 2.6 | 3.1 | -6.7 | -4.0 | -4.5 | -4.6 |
| WLSv-subset | -51.6 | -32.7 | -36.6 | -29.6 | -18.3 | -9.8 | -10.5 | -10.9 | -1.1 | -4.3 | -8.1 | -7.3 | 2.5 | 2.1 | 2.3 | 1.8 | -7.9 | -4.3 | -5.8 | -6.5 |
| WLSv-intuitive | -60.6 | -29.1 | -41.4 | -36.6 | -14.5 | -8.7 | -5.6 | -4.8 | -3.3 | -6.8 | -8.0 | -7.0 | 5.5 | 2.6 | 2.6 | 3.1 | -6.7 | -4.0 | -4.5 | -4.6 |
| WLSv-lasso | -60.6 | -29.1 | -41.4 | -36.6 | -14.5 | -8.7 | -5.6 | -4.8 | -3.3 | -6.8 | -8.0 | -7.0 | 5.5 | 2.6 | 2.6 | 3.1 | -6.7 | -4.0 | -4.5 | -4.6 |
| MinTs | -27.0 | -21.1 | -22.9 | -21.8 | -9.1 | -7.9 | -6.7 | -4.6 | -3.6 | -9.0 | -10.5 | -7.6 | 7.7 | 3.7 | 3.0 | 3.4 | -1.9 | -3.3 | -3.9 | -3.1 |
| MinTs-subset | -41.4 | -9.3 | -17.8 | -45.1 | -12.2 | -5.0 | -8.2 | -6.8 | -6.1 | -9.8 | -7.1 | -9.3 | 5.3 | 4.7 | 3.8 | 3.6 | -5.3 | -1.5 | -3.0 | -6.1 |
| MinTs-intuitive | -27.0 | -21.1 | -22.9 | -21.8 | -9.1 | -7.9 | -6.7 | -4.6 | -3.6 | -9.0 | -10.5 | -7.6 | 7.7 | 3.7 | 3.0 | 3.4 | -1.9 | -3.3 | -3.9 | -3.1 |
| MinTs-lasso | -27.0 | -21.1 | -22.9 | -21.8 | -9.1 | -7.9 | -6.7 | -4.6 | -3.6 | -9.0 | -10.5 | -7.6 | 7.7 | 3.7 | 3.0 | 3.4 | -1.9 | -3.3 | -3.9 | -3.1 |
| EMinT | -60.4 | -14.0 | 1.4 | -29.9 | -6.0 | 12.0 | 10.7 | -6.7 | 16.7 | -0.9 | -12.4 | -21.0 | 23.3 | 17.2 | 16.7 | 10.1 | 7.7 | 10.8 | 9.0 | -3.7 |
| Elasso | -4.2 | -3.3 | -22.3 | -8.0 | -19.7 | -9.9 | -19.9 | -25.3 | -24.6 | -24.3 | -22.6 | -14.6 | -10.8 | -3.8 | -0.2 | -4.9 | -15.7 | -9.3 | -11.4 | -13.2 |

Table 13: Number of time series selected using different proposed methods and the optimal parameter values identified in the labour application.

| | Number of time series retained | | | | | Optimal parameters | | |
|--------------|--------------------------------|----------|-----|----------------|-------|--------------------|-------------|-------------|
| | Top | Duration | STT | Duration x STT | Total | λ | λ_0 | λ_2 |
| None | 1 | 6 | 8 | 48 | 63 | - | - | - |
| OLS-subset | 0 | 5 | 1 | 48 | 54 | - | 4.16 | 1.00 |
| WLSs-subset | 0 | 5 | 1 | 46 | 52 | - | 0.38 | 0.10 |
| WLSv-subset | 1 | 5 | 7 | 48 | 61 | - | 0.51 | 1.00 |
| MinTs-subset | 0 | 1 | 1 | 47 | 49 | - | 0.03 | 0.01 |
| Elasso | 1 | 5 | 2 | 3 | 11 | 213.59 | - | - |

forecast reconciliation. Remarkably, the Elasso method consistently outperforms the others overall, even though it uses only 11 series for forecast reconciliation. Additionally, it is worth noting that most of the series at the STT level are removed, while the majority of series at the Duration level are retained. This aligns with our data description, highlighting that the seasonal patterns in the Duration level series is more consistent and potentially easier to forecast compared to those at the STT level.

6 Conclusion

In the existing literature on hierarchical time series and linear forecast reconciliation, we map all base forecasts into bottom-level disaggregated forecasts, which are then summed up by a summing matrix to yield coherent forecasts for the entire structure. Hence, the mapping step in forecast reconciliation can be conceptually regarded as a forecast combination. In practical applications, it is common that the base forecasts for some time series in the hierarchical structure may perform poorly, especially in the context of large hierarchies. This may reduce the overall effectiveness of forecast reconciliation methods. In this paper, we aimed to address this issue by introducing a selection mechanism in forecast reconciliation, i.e., involving time series selection when reconciling forecasts for hierarchical time series while ensuring the generation of coherent forecasts for all series.

Under the unbiasedness constraint, we developed three reconciliation methods with selection mechanisms to keep forecasts for an automatically selected set of series unused in forming reconciled forecasts. These methods include group best-subset selection with ridge regularization (Subset), intuitive method with L_0 regularization (Intuitive), and group lasso method (Lasso). These methods formulated the problem based on out-of-sample base forecasts using different penalty functions designed to penalize the columns of the weighting matrix, G , towards zero. Additionally, we relaxed the unbiasedness constraint and proposed the empirical group lasso method (Elasso) which achieves series selection based on in-sample observations and fitted values.

The simulation experiments and two empirical applications demonstrated the superiority of the proposed methods over the reconciliation methods that do not involve series selection. In particular, when model misspecification was introduced for some series in the hierarchy, our proposed methods guaranteed coherent forecasts that outperformed or, at the very least, matched their respective benchmark methods in the minimum trace reconciliation framework. In both empirical applications, where no apparent model misspecification was present, the Subset and Elasso methods were always preferred, while the Intuitive and Lasso methods yield results identical to the corresponding benchmark methods, as they tend to provide dense estimates.

A remarkable feature of the proposed methods is their ability to reduce the disparities arising from using different estimates of the base forecast error covariance matrix W , thereby mitigating the challenges associated with estimator selection, which is a prominent issue within the field of forecast reconciliation research.

Acknowledgement

References

- Athanasopoulos, G, RA Ahmed & RJ Hyndman (2009). Hierarchical forecasts for Australian domestic tourism. *International Journal of Forecasting* **25**(1), 146–166.
- Athanasopoulos, G, RJ Hyndman, N Kourentzes & A Panagiotelis (2023). Forecast reconciliation: A review. URL: robjhyndman.com/publications/hfreview.html.
- Athanasopoulos, G, RJ Hyndman, N Kourentzes & F Petropoulos (2017). Forecasting with temporal hierarchies. *European Journal of Operational Research* **262**(1), 60–74.
- Ben Taieb, S & B Koo (2019). Regularized Regression for Hierarchical Forecasting Without Unbiasedness Conditions. In: *Proceedings of the 25th ACM SIGKDD International Conference on Knowledge Discovery & Data Mining*. KDD '19. Anchorage, AK, USA: Association for Computing Machinery, pp.1337–1347.
- Bertsimas, D, A King & R Mazumder (2016). Best subset selection via a modern optimization lens. en. *The Annals of Statistics* **44**(2), 813–852.
- Di Fonzo, T & D Girolimetto (2023). Cross-temporal forecast reconciliation: Optimal combination method and heuristic alternatives. *International Journal of Forecasting* **39**(1), 39–57.
- Dunn, DM, WH Williams & TL Dechaine (1976). Aggregate versus Subaggregate Models in Local Area Forecasting. *Journal of the American Statistical Association* **71**(353), 68–71.
- Erven, T van & J Cugliari (2015). Game-Theoretically Optimal Reconciliation of Contemporaneous Hierarchical Time Series Forecasts. In: *Modeling and Stochastic Learning for Forecasting in High Dimensions*. Springer International Publishing, pp.297–317.
- Gross, CW & JE Sohl (1990). Disaggregation methods to expedite product line forecasting. en. *Journal of Forecasting* **9**(3), 233–254.
- Hazimeh, H & R Mazumder (2020). Fast Best Subset Selection: Coordinate Descent and Local Combinatorial Optimization Algorithms. *Operations Research* **68**(5), 1517–1537.
- Hazimeh, H, R Mazumder & P Radchenko (2023). Grouped variable selection with discrete optimization: Computational and statistical perspectives. en. *The Annals of Statistics* **51**(1), 1–32.
- Hazimeh, H, R Mazumder & A Saab (2022). Sparse regression at scale: branch-and-bound rooted in first-order optimization. *Mathematical Programming* **196**(1), 347–388.
- Hyndman, RJ, RA Ahmed, G Athanasopoulos & HL Shang (2011). Optimal combination forecasts for hierarchical time series. *Computational Statistics & Data Analysis* **55**(9), 2579–2589.

- Hyndman, RJ, G Athanasopoulos, C Bergmeir, G Caceres, L Chhay, M O'Hara-Wild, F Petropoulos, S Razbash, E Wang & F Yasmeeen (2023). *forecast: Forecasting functions for time series and linear models*. R package version 8.21.1. <https://pkg.robjhyndman.com/forecast/>.
- Hyndman, RJ, AJ Lee & E Wang (2016). Fast computation of reconciled forecasts for hierarchical and grouped time series. *Computational Statistics & Data Analysis* **97**, 16–32.
- Mazumder, R, P Radchenko & A Dedieu (2022). Subset Selection with Shrinkage: Sparse Linear Modeling When the SNR Is Low. *Operations Research*.
- Nystrup, P, E Lindström, P Pinson & H Madsen (2020). Temporal hierarchies with autocorrelation for load forecasting. *European Journal of Operational Research* **280**(3), 876–888.
- Panagiotelis, A, G Athanasopoulos, P Gamakumara & RJ Hyndman (2021). Forecast reconciliation: A geometric view with new insights on bias correction. *International Journal of Forecasting* **37**(1), 343–359.
- Pritularga, KF, I Svetunkov & N Kourentzes (2021). Stochastic coherency in forecast reconciliation. *International Journal of Production Economics* **240**, 108221.
- Taieb, SB, JW Taylor & RJ Hyndman (2021). Hierarchical Probabilistic Forecasting of Electricity Demand With Smart Meter Data. *Journal of the American Statistical Association* **116**(533), 27–43.
- Wickramasuriya, SL (2023). Probabilistic forecast reconciliation under the Gaussian framework. *Journal of Business & Economic Statistics*.
- Wickramasuriya, SL (2021). Properties of point forecast reconciliation approaches. arXiv: [2103.11129 \[stat.ME\]](#).
- Wickramasuriya, SL, G Athanasopoulos & RJ Hyndman (2019). Optimal Forecast Reconciliation for Hierarchical and Grouped Time Series Through Trace Minimization. *Journal of the American Statistical Association* **114**(526), 804–819.
- Yuan, M & Y Lin (2006). Model selection and estimation in regression with grouped variables. *Journal of the Royal Statistical Society. Series B, Statistical Methodology* **68**(1), 49–67.